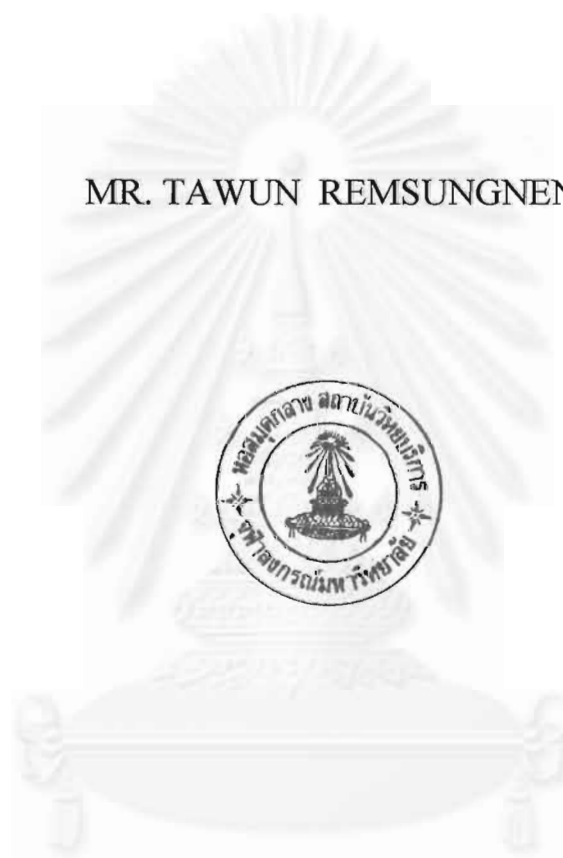


MOLECULAR DYNAMICS SIMULATION OF  
CONCENTRATED LITHIUM-LIQUID AMMONIA SOLUTIONS  
USING A PSEUDOPOTENTIAL

MR. TAWUN REMSUNGREN



A Thesis Submitted in Partial Fulfillment of the Requirements  
for the Degree of Master of Science in Computational Science  
Department of Mathematics

Graduate School

Chulalongkorn University

Academic Year 1999

ISBN 974-332-869-6

๕ ๑๙๖๑๙๑๖๕

การจำลองทางพลวัตเชิงโมเลกุลสำหรับสารละลาย

ลิเทียมไอออนในแอมโมเนียเหลว ที่เข้มข้น โดยใช้ศักย์เทียม



วิทยานิพนธ์นี้เป็นส่วนหนึ่งของการศึกษาตามหลักสูตรปริญญาวิทยาศาสตรมหาบัณฑิต

สาขาวิทยาการคอมพิวเตอร์ ภาควิชาคณิตศาสตร์  
บัณฑิตวิทยาลัย จุฬาลงกรณ์มหาวิทยาลัย

ปีการศึกษา 2542

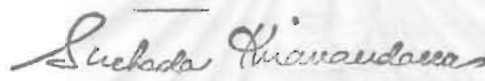
ISBN 974-332-869-6

ลิขสิทธิ์ของบัณฑิตวิทยาลัย จุฬาลงกรณ์มหาวิทยาลัย

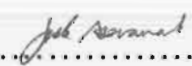
Thesis Title        Molecular Dynamics Simulations Of Concentrated  
Lithium- Liquid Ammonia Solution With A  
Pseudopotential  
By                     Mr. Tawun Remsungnen  
Department         Mathematics  
Thesis Advisor     Associate Professor Supot Hannongbua, Ph.D.


---

Accepted by Graduate School, Chulalongkorn University in Partial  
Fulfillment of Requirement for the Master's Degree.

  
.....Dean of Graduate school  
(Associate Professor Suchada Kiranandana, Ph.D.)

Thesis Committee

  
.....Chairman  
(Assistant Professor Jack Asavanant, Ph.D.)

  
.....Thesis Advisor  
(Associate Professor Supot Hannongbua, Ph.D.)

  
.....Member  
(Associate Professor David Ruffolo, Ph.D.)

เทวัญ เริ่มสูงเนิน: การจำลองทางพลศาสตร์เชิงโมเลกุลของสารละลาย ลิเธียม  
ไอออนในแอมโมเนียเหลวที่เข้มข้น โดยใช้ศักย์เทียม (MOLECULAR DYNAMICS  
SIMULATION OF CONCENTRATED LITHIUM-LIQUID AMMONIA SOLUTIONS  
USING A PSEUDOPOTENTIAL) อ. ที่ปรึกษา: รศ. ดร. สุพจน์ หารหนองบัว,  
60 หน้า. ISBN 974-332-869-6

ได้ทำการจำลองทางพลวัตเชิงโมเลกุลสำหรับสารละลายลิเธียมไอออนในแอมโมเนีย  
เหลวที่เข้มข้น ที่อุณหภูมิเฉลี่ย 241 เคลวิน ก่อสร้างลูกบาศก์บรรจุ 50 ลิเธียมไอออน 50 อิเล็กตรอน  
และ 205 โมเลกุลแอมโมเนีย โดยใช้ข้อมูลความหนาแน่นที่ได้จากการทดลองซึ่งมีค่า 0.498 กรัมต่อ  
ลูกบาศก์เซนติเมตร ทำให้คำนวณความยาวกล่องได้ 23.39 อังสตรอม อันตรกิริยาระหว่างอนุภาคที่  
ทำการจำลองแบบ แทนด้วยทั้งศักย์ฟังก์ชันที่สร้างขึ้นจากการคำนวณทางเคมีควอนตัมโดยตรง และ  
ศักย์เทียมซึ่งอธิบายผลกระทบของอิเล็กตรอนอิสระที่ละลายอยู่ในสารละลาย โดยในการศึกษานี้ใช้  
ศักย์เทียม 2 แบบ ผลการศึกษาพบว่า ไอออนลิเธียมถูกซอลเวตด้วยแอมโมเนีย 6 โมเลกุล โครงสร้าง  
ของตัวทำละลายเปลี่ยนแปลงอย่างสิ้นเชิง เมื่อเปรียบเทียบกับแอมโมเนียเหลวบริสุทธิ์ กลุ่มก้อน  
ขนาดใหญ่  $Li_n(NH_3)_n^+$  และการใช้แอมโมเนียร่วมกันของไอออนลิเธียม 2, 3 และ 4 ไอออนถูกตรวจ  
พบ ผลสืบเนื่องจากการเกิดกลุ่มก้อนคือได้เกิดช่องว่างขนาดใหญ่ขึ้นในสารละลาย

จุฬาลงกรณ์มหาวิทยาลัย

ภาควิชา .....  
สาขาวิชา .....  
ปีการศึกษา .....

ลายมือชื่อนิสิต .....  
ลายมือชื่ออาจารย์ที่ปรึกษา .....  
ลายมือชื่ออาจารย์ที่ปรึกษาร่วม .....

## : MAJOR COMPUTATIONAL SCIENCE  
KEY WORD: MOLECULAR DYNAMICS SIMULATIONS / METAL-AMMONIA  
SOLUTION / PSEUDOPOTENTIAL

TAWUN REMSUNGREN: MOLECULAR DYNAMICS SIMULATION  
OF CONCENTRATED LITHIUM-LIQUID AMMONIA SOLUTIONS  
USING A PSEUDOPOTENTIAL. THESIS ADVISORS: ASSOC. PROF.  
SUPOT HANNONGBUA, Ph.D. 60pp ISBN 974-332-869-6

Molecular dynamics simulations of a concentrated lithium-liquid ammonia solution have been performed at an average temperature of 241 K. The basic cube contains 50  $\text{Li}^+$ , 50 delocalized electrons and 205  $\text{NH}_3$  (19.58 mole percent of lithium ions). With an experimental density of  $0.498 \text{ g.cm}^{-3}$ , a side-length of a periodic cube of  $23.39 \text{ \AA}$  was obtained. Interactions between particles in the simulation cube were described by the direct and indirect potentials. The first function was developed using quantum chemical calculations while the second one, which represents the effect of free electrons dissolved in the solution, was evaluated based on pseudopotential theory. Two pseudopotential models were employed in this study. The results show that the lithium ion was solvated by six ammonia molecules. The solvent structure was completely changed in comparison with that observed for pure liquid ammonia. Big clusters of  $\text{Li}_m(\text{NH}_3)_n^+$  sharing of one ammonia molecule by 2, 3 and 4 lithium ions have been detected. As a consequence of the cluster formation, big cavities are formed in the solution.

สถาบันวิทยบริการ  
จุฬาลงกรณ์มหาวิทยาลัย

ภาควิชา.....คณิตศาสตร์.....

สาขาวิชา.....วิชาการคหฬ.....

ปีการศึกษา.....๒๕๔๒.....

ลายมือชื่อนิสิต..... T. Remsungren.....

ลายมือชื่ออาจารย์ที่ปรึกษา..... S. Hannbua.....

ลายมือชื่ออาจารย์ที่ปรึกษาร่วม.....

## ACKNOWLEDGMENTS



This thesis was made completely and fast with full speed ahead helping of my kindful advisor, Associate Professor Supot Hannongbua. I would like to express my deep gratitude to him for his guiding, advising, understanding and encouraging. I owe a great dept of gratitude to my co-advisor, Prof. K. Heinzinger from Max-Plank Institute for Chemie, Germany and Prof. Z. Kurskii from Institute for Physics of Condensed Matter, Ukraine.

In addition, I am grateful to Austrian-Thai Centre for Computer Assisted Chemical Education and Research for computer resource supplements. Financial supports by Austrian Ministry of Foreign Affairs and Graduate School are also gratefully acknowledged. I wish to thank all faculty members of Computational Science Program.

Finally, I would like to give my gratitude to my parents for their understanding encouragement and continuous supporting during the whole studying.

จุฬาลงกรณ์มหาวิทยาลัย

# CONTENTS

<b>ABSTRACT IN THAI</b> .....	iv
<b>ABSTRACT IN ENGLISH</b> .....	v
<b>ACKNOWLEDGMENT</b> .....	vi
<b>CONTENTS</b> .....	vii
<b>LIST OF FIGURES</b> .....	ix
<b>LIST OF TABLES</b> .....	xi
<b>CHAPTER 1 INTRODUCTION</b> .....	<b>1</b>
1.1 Computational Science: The Third Method of Science! .....	1
1.2 Computer Simulations in Chemistry .....	2
1.3 A Non-aqueous Solvent System .....	2
1.4 Summary of This Work .....	3
<b>CHAPTER 2 QUANTUM THEORY</b> .....	<b>4</b>
2.1 Quantum Mechanics Methods .....	4
2.2 Schrödinger Equation .....	6
2.3 Born-Oppenheimer Approximation .....	7
2.4 Linear Combinations of Atomic Orbitals (LCAO) Approximation .....	8
2.5 Basis Functions .....	9
2.6 Hartree-Fock Theory and Hartree-Fock Self-consistent-field Method .....	10
2.7 Basis Set Superposition Error .....	14
<b>CHAPTER 3 MOLECULAR DYNAMICS SIMULATION</b> .....	<b>15</b>
3.1 What is Molecular Dynamics? .....	15
3.2 Historical Molecular Dynamics .....	16
3.3 Molecular Dynamics Procedure .....	18

3.3.1 The Predictor-Corrector Algorithm.....	20
3.3.2 Periodic Boundary Conditions .....	21
3.3.3 Cut-Off Limit .....	22
3.3.4 Long-Range Interactions .....	22
3.3.5 Shifted and Shifted-Force Potentials.....	23
3.4 Calculation of Macroscopic Properties .....	23
3.4.1 Structural Properties.....	23
3.4.2 Dynamical Properties .....	24
<b>CHAPTER 4 DETAIL OF CALCULATIONS .....</b>	<b>26</b>
4.1 Simulation Models .....	26
4.1.1 Total Energy .....	26
4.1.2 Ammonia Intramolecular Potential .....	27
4.1.3 Intermolecular Potentials.....	29
4.2 Molecular Dynamics Simulation.....	32
<b>CHAPTER 5 RESULT AND DISCUSSION .....</b>	<b>33</b>
5.1 Pair Potentials and Pseudopotential Effects.....	33
5.2 Structural Properties.....	36
5.3 Dynamical Properties .....	47
<b>CHAPTER 6 CONCLUSIONS .....</b>	<b>51</b>
<b>REFERENCES .....</b>	<b>53</b>
<b>APPENDIX .....</b>	<b>55</b>
<b>CURRICULUM VITAE .....</b>	<b>60</b>



## LIST OF FIGURES

<b>Figure 1.1</b>	The connection between experiment, theory, and computer simulation.....	3
<b>Figure 3.1</b>	The scheme in molecular dynamics simulation. ....	19
<b>Figure 5.1</b>	Total site-site potentials as a function of the distances for the six different interactions, calculated from models I (solid line) and model II (dotted line). The dashed line denotes direct interactions.....	34
<b>Figure 5.2</b>	Ammonia-ammonia (a) and lithium-ammonia (b) pair potentials as a function of nitrogen-nitrogen and lithium-nitrogen distances, for the orientations shown in the inserts. The dashed line gives the potential of direct interaction. Solid and dotted lines are the total potentials obtained from model I and II, respectively. ....	35
<b>Figure 5.3</b>	Lithium-lithium (a) and lithium-ammonia (b) pair potentials taken from literatures. Solid lines are from Hannongbua et al., [1992] and dotted lines from Hannongbua et al. [1997].....	35
<b>Figure 5.4</b>	Snapshot of the 19.58 mole percent of lithium ions in liquid ammonia using the pseudopotential (a) model I and (b) model II. The single red balls represent lithium ions. The white together with blue balls denote ammonia molecules (white for hydrogen and blue for nitrogen). The largest orange balls are insert in order to mark the corners of the simulation box.....	37
<b>Figure 5.5</b>	Ammonia-ammonia radial distribution functions and their integration numbers obtained from the simulations using pseudopotential (a) model I and (b) model II. ....	38
<b>Figure 5.6</b>	Lithium-ammonia radial distribution functions and their integration number obtained from the simulation using pseudopotential (a) model I and (b) model II. ....	41

<b>Figure 5.7</b>	Distribution of $\cos \mu$ where $\mu$ is defined as the nitrogen-lithium-nitrogen angle calculated for the ammonia molecules in the solvation shell of the lithium ions. Solid and dotted lines were obtained from model I and II, respectively.....	43
<b>Figure 5.8</b>	Distribution of $\cos \alpha$ for ammonia molecules in the solvation shell of lithium ions. The solid and dashed lines were obtained from the simulations using pseudopotential models I and II, respectively.....	43
<b>Figure 5.9</b>	Snapshot which show that one ammonia molecule was shared by 2, 3 or 4 lithium ions (nitrogen-lithium distances $\leq 2.5 \text{ \AA}$ ).....	44
<b>Figure 5.10</b>	The electron density of a representative configuration of a cesium-ammonia solution at high electron concentration. The system consists of 24 cesium ions in 256 ammonia molecules [Klein 1994].....	46
<b>Figure 5.11</b>	Normalized center-of-mass velocity autocorrelation functions for ammonia molecules in the bulk (dashed line) and in the solvation shell (full line) of lithium for (a) model I and (b) model II.....	47
<b>Figure 5.12</b>	Spectral density of the translational motions of the normalized center of mass velocity autocorrelation functions shown in Figure 5.11 for ammonia molecules in the bulk (black line) and in the first solvation shell (blue line) of lithium obtained from the simulations for (a) model I and (b) model II.....	48
<b>Figure 5.13</b>	Spectral density of the rotation about x- (full line), y- (dashed line) and z-axes (dotted line) for ammonia molecules in the bulk (a) and in the solvation shell of lithium (b) obtained from model I.....	49
<b>Figure 5.14</b>	Spectral density of the rotation about x- (full line), y- (dashed line) and z-axes (dotted line) for ammonia molecules in the bulk (a) and in the solvation shell of lithium (b) obtained from model II.....	49
<b>Figure 5.15</b>	Asymmetric stretching and bending spectral densities obtained from the simulation using pseudopotential (a) model I and (b) model II.....	50
<b>Figure A.1</b>	Procedural detail of MAIN program.....	56

## LIST OF TABLES

<b>Table 4.1</b>	Directed intermolecular potentials employed in simulation. Energies are given in units of $10^{-19}$ J with the distances in Å. ....	30
<b>Table 4.2</b>	Parameter potential functions for the Li-ammonia pair potentials function the energy are given in $\text{kJ mol}^{-1}$ with R in Å. ....	30
<b>Table 5.1</b>	Characteristic values of the radial distribution functions, $g_{\alpha\beta}(r)$ for the lithium – ammonia solution. $r_{M1}$ , $r_{M2}$ and $r_{m1}$ are distances in Å where, $g_{\alpha\beta}(r)$ has first and second maximum and first minimum, respectively, $n_{\alpha\beta}(r_{m1})$ is running integration numbers, integrated up to $r_{m1}$ . Those values for the dilute solution, 0.46 mole percent, are also given, in parenthesis, for comparison.. ....	42
<b>Table 5.2</b>	Percentage of nearest neighbor lithium ions, $n_{\text{LiLi}}(R_{m1})$ , around a central one. ....	42
<b>Table 5.3</b>	The fraction in % of the cluster of kind m .....	45
<b>Table 5.4</b>	Comparison of various vibrational frequencies calculated from the simulaion separately for ammonia molecules in the first solvation shell of lithium ions, the bulk liquid, and in the gas phase with experimental results. ....	50

# CHAPTER 1

## INTRODUCTION



### 1.1 Computational Science: The Third Method of Science!

Today computer technology has rapidly developed and plays a very important role in many fields in science, including studies and research. In the past, physical properties were characterized by experiments and theories. In experiment, a system is subjected to measurements and results. In theory, a model of the system is developed in form of a set of mathematical equations. '*Computational Science*' makes use of numerical computations and graphic visualization evaluating interested-informations of new scientific investigations.

As such, computational science must be separated from computer science. *Computer science* playing on the computer itself, it is the science and engineering of computer systems, including hardware and software. On the other hand, *Computational Science* is interdisciplinary. It uses the technology of the computer to study problems in mathematics, physics, chemistry, biology, other applied science and engineering fields. A computational scientist needs to be conversant in both the fundamentals of computer science and in the scientific field whose problems he wishes to solve.

Computational science techniques are used to simulate physical events and to process large amounts of generated or collected data. The use of simulation in research and development is now established as a third basic methodology of doing scientific research, in addition to theory and experiment. The importance of computer simulation is illustrated by the *grand challenge*, *new drug design* and *new product design* problems, whose solution is beneficial to society but will require vastly more powerful computers and more scientists in this.

## 1.2 Computational Simulations in Chemistry

Models of chemical systems and specialized theoretical chemistry are mainly constructed in the form of quantum chemical calculations and statistical mechanics simulations. These tools are widely applicable for many systems, especially for investigation of microscopic properties and lead directly and perhaps easily to a set of interesting results or macroscopic properties of the system. The result of computer simulation can be directly compared with those of real experiment.

Computational simulations can fill the gap between theory and experiment. If the model is good, it is expected that the simulation results are compatible with experimental results. On the other hand, the predictions of some complicated theoretical models can also be tested with simulation results. The connection between experiment, theory, and computer simulations is shown in Figure 1.1.

Computer simulation methods, such as **Monte Carlo (MC)** practically introduced by Metropolis [1953], and **Molecular Dynamics (MD)**, introduced by Alder [1960], are widely tools for studying statistical and dynamical properties of liquid and solutions. Both simulation methods can be used to evaluate structural properties of systems, included some data inaccessible by experimental techniques. However, Molecular Dynamics methods show not only the structural properties but can also calculate dynamical properties of the system.

## 1.3 A Non-Aqueous Solvent System

A non-aqueous solvent of widespread interest is liquid ammonia. Interest is focussed on its solution of alkali or alkali earth metals because of there remarkable properties such as high electrical conductivity [Lepoutre and Seinko 1964]. In region of high metal-concentrations, the solutions behave like liquid metal while their free-electron densities are much lower compared to pure metal [Thompson 1976]. Metal solution in liquid ammonia consists of ammonia molecules, metal ions and free

(conduction) electrons. The presence of free electrons is a special feature of metal ammonia systems. Here electrons must be treated as quantum particles. This gives rise to considerable difficulties in computer simulations of liquid metal-ammonia solutions.

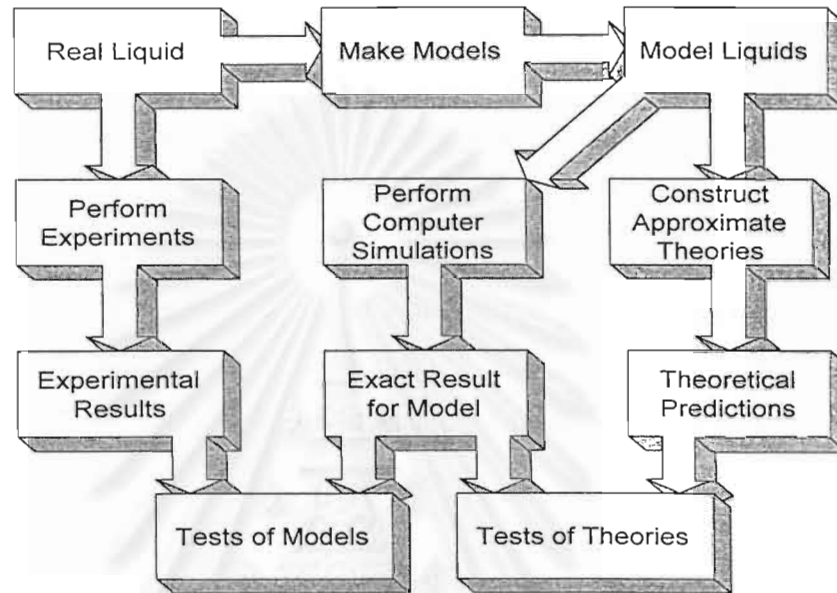


**Figure 1.1** The connection between experiment, theory and computer simulations [Allen and Tildesley, 1987].

## 1.4 Summary of This Work

By the application of pseudopotential theory, new effective interatomic potentials are derived. Aim of this study is to use classical computer simulation methods to calculate structural and dynamical properties of concentrated metal-ammonia solutions where free electron can be excluded from explicit consideration. The metal ion that used in this study is lithium ion. Simulations have been carried out at highest concentrations of this solution (19.58 mole percent of lithium ions in liquid ammonia).

## CHAPTER 2

# QUANTUM THEORY

Quantum chemistry is highly mathematical method and the language used to describe quantum mechanics more often relates to equations than to chemical concepts. The system is described by a wavefunction which can be obtained by solving the Schrödinger equation [Schrödinger, 1926]. This equation relates the stationary states of the system and their energies to the Hamiltonian operator, which can be viewed as the recipe for obtaining the energy associated with a wavefunction describing the positions of the nuclei and electrons in the system. In practice, the Schrödinger equation cannot be solved exactly and approximations have to be made. Quantum mechanics are nowadays substantially applied in all branches of chemistry, both theoretical and experimental investigations.

### 2.1 Quantum Mechanics Methods

Quantum mechanics methods are based on the following principles;

- Nuclei and electrons are distinguished from each other,
- Electron-electron and electron-nuclear interactions are explicit,
- Interaction are governed by nuclear and electron charges and electron motions,
- Interaction determines the spatial distribution of nuclei and electrons and their energy.

To obtain a numerical approximated solution of the Schrödinger equation, all electrons in the system will be treated using one-electron wavefunctions called spin orbitals. These spin orbitals will be combined to form the many-electron

wavefunction. This technique is called **molecular orbital (MO)** theory. There are two categories: semiempirical and *ab initio* methods.

### *Ab initio*

- Use the full Hamiltonian and do not use experimental data other than the values of fundamental physical constants,
- Limited to about 100 atoms best performed using a high performance computer and can be applied to all kind of molecule, and molecular fragments,
- Vacuum or implicit solvent environment,
- Can be used to study ground, transition, and excited states.

### Semiempirical

- Use a simpler Hamiltonian and some of the time consuming mathematical terms in Schrödinger Equation. The parameters can be derived from experimental measurements or by performing *ab initio* calculations,
- Limited to some hundred atoms,
- Can be applied to mostly only to organic molecules, including small oligomers,
- Can be used to study ground, transition, and excited states.



## 2.2 Schrödinger Equation

System in quantum mechanics, the energy and many properties of stationary state of molecule can be obtained by solution of wavefunction, which satisfies the Schrödinger equation,

$$i\hbar \frac{\partial}{\partial t} \Psi(\vec{r}, t) = \left( -\frac{\hbar^2}{2m} \nabla^2 + V(\vec{r}) \right) \Psi(\vec{r}, t). \quad (2.1)$$

If the potential  $V(\vec{r})$  is not explicitly time-dependent, and for appropriate boundary conditions, we can find a separable solution, so that the wave function can be written as

$$\Psi(\vec{r}, t) = \psi(\vec{r}) e^{-iEt/\hbar}, \quad (2.2)$$

where  $E$  is interpreted as the energy, which leads to the time-independent Schrödinger equation

$$E \psi(\vec{r}) = \left( -\frac{\hbar^2}{2m} \nabla^2 + V(\vec{r}) \right) \psi(\vec{r}) = \mathbf{H} \psi(\vec{r}), \quad (2.3)$$

where  $\psi(\vec{r})$  is the *normalized wavefunction* of the system and  $\mathbf{H}$  is called the *Hamiltonian operator*, representing the energy. However, in the case of the many electron problem, the solution of the problem must also include the *Pauli's exclusion principle*, that any pair of electrons with respect to the interchange of the coordinates, their wavefunction must be antisymmetric.

For some systems which consist of one electron, it is easily to solve in order to obtain an exact solution of the Schrödinger equation, but all case of many-electron systems, only approximate solutions can be achieved, then approximation techniques and procedures are needed and implemented.

### 2.3 Born-Oppenheimer Approximation: Separation of Nuclei Motion

Born-Oppenheimer approximation suppose that electrons mass is very much smaller than the mass of the nuclei. Therefore, the nuclear motion is much slower than electrons. That reason why one can separate the nuclear and electron translation parts of the Schrödinger equation. It is also approximate that the force and potential acting on the electrons depend on the fixed positions of nuclei, that is and the approximately average value over several electron interactions with nuclei.

$$\mathbf{H}\psi(\vec{r}, \vec{R}) = E\psi(\vec{r}, \vec{R}), \quad (2.4)$$

with the Hamiltonian operator written as

$$\mathbf{H} = \mathbf{T}_n + \mathbf{V}_n + \mathbf{H}_e, \quad (2.5)$$

where

$$\mathbf{V}_n = \sum_{A < B} \frac{Z_A \cdot Z_B}{R_{AB}}$$

$$\mathbf{T}_n = - \sum_{\text{all nuclei}} \frac{1}{2M_n} \nabla_n^2 \quad \text{and} \quad \mathbf{H}_e = - \sum_i \frac{1}{2} \nabla_i^2 - \sum_{iA} \frac{Z_A}{r_{iA}} + \sum_{i < j} \frac{1}{r_{ij}}.$$

By assume that the solution of the Schrödinger equation can be separated into the form,

$$\psi(\vec{r}, \vec{R}) = \Phi(\vec{r}, \vec{R})\chi(\vec{R}), \quad (2.6)$$

and the Schrödinger equation will also be separated into two equations, for the electronic wavefunction,

$$[\mathbf{H}_e + \mathbf{V}_n(\vec{R})]\Phi(\vec{r}, \vec{R}) = U(\vec{R})\Phi(\vec{r}, \vec{R}) \quad (2.7)$$

and for the nuclear motion.

$$[\mathbf{T}_n + U(\vec{R})]\chi(\vec{R}) = E\chi(\vec{R}) \quad (2.8)$$

It can be seen that the potential term  $U(\vec{R})$  depends on only the position of the nuclei. This is used for an important construct known as the potential energy surface.

## 2.4 Linear Combinations of Atomic Orbitals (LCAO) Approximation

Linear Combinations of Atomic Orbitals is involved in the calculation for approximately solve the electronic Schrödinger equation. The main idea of this approximation is to suppose that individual molecular wavefunction can be obtained from linear combination of a finite set of one-electron wavefunctions called the *basis set*,  $\phi$ , and write in the form

$$\chi_i(x) = \sum_{\mu=1}^N c_{\mu i} \phi_{\mu}(x) \quad (2.9)$$

where  $c_{\mu i}$  are the molecular orbital expansion coefficients. Then the one-electron functions are brought together to approximate the full wavefunction  $\psi(x_1, x_2, \dots, x_N)$  in form of Slater determinant:

$$\Psi^{n\text{-ele}} = \frac{1}{\sqrt{n!}} \begin{vmatrix} \chi_1(x_1) & \chi_1(x_2) & \chi_1(x_3) & \cdots & \chi_1(x_n) \\ \chi_2(x_1) & \chi_2(x_2) & \cdots & \cdots & \cdots \\ \vdots & \vdots & & & \vdots \\ \chi_n(x_1) & \cdots & \cdots & \cdots & \chi_n(x_n) \end{vmatrix} \quad (2.10)$$

where  $x_i = (\vec{r}_i, \omega_i)$ ,  $\vec{r}_i$  is the space coordinate and  $\omega_i$  is the spin coordinate. Then the electronic energy can be calculated from

$$E = \langle \Psi | \mathbf{H}_e | \Psi \rangle. \quad (2.11)$$

## 2.5 Basis Functions

Two types of basis functions named Slater Type Orbitals (STO) and Gaussian Type Orbitals (GTO), are normally used to represent the primitive functions  $\phi_{\mu}(x)$ , for convenient one-electron wavefunction or spin orbitals  $\chi_i(x_i)$ .

### 2.5.1 Slater-type atomic orbitals, STO

This set of functions is derived from exact solutions in the case of the hydrogen atom, with general form as [Slater, 1930]

$$\phi_{\text{STO}}(n, l, m, \zeta) = |\vec{r}|^{n-1} \exp(-\zeta|\vec{r}|) Y_{lm}(\theta, \phi). \quad (2.12)$$

It is usually used for small systems. Functions of this type yield a very good approximation for orbital wavefunctions and produce good results of calculations. However, the exponential term in the function causes some difficulties to evaluate numerical integrals.

### 2.5.2 Gaussian-type atomic orbital, GTO

Functions of this type were introduced into molecular orbital computations by Boy [1950]. Their general form can be written as

$$\phi_{\text{GTO}}(\lambda, \mu, \nu, \alpha) = x^{\lambda} y^{\mu} z^{\nu} \exp(-\alpha|\vec{r}|^2). \quad (2.13)$$

They are less satisfactory than STO in representing atomic orbitals, because they do not have a cusp at the origin. However, the advantage of this type of function is that all integrals in the computations can be evaluated without numerical integration.

## 2.6 Hartree –Fock Theory and Hartree-Fock Self-Consistent-Field Method

Hartree-Fock theory is the variational method which is one of the standard techniques used in quantum mechanics. Hartree-Fock theory seeks the optimized energy for the system under consideration. The Hamiltonian operator for many electrons can be written as

$$\mathbf{H} = \sum_k \frac{-\hbar^2}{2m} \nabla_k^2 + \frac{1}{2} \sum_{k,l} \frac{e^2}{|\vec{r}_k - \vec{r}_l|}, \quad (2.14)$$

which can be separated into two components,

$$\mathbf{H} = \mathbf{H}_1 + \mathbf{H}_2 \quad (2.15)$$

where

$$\mathbf{H}_1 = \sum_k \frac{-\hbar^2}{2m} \nabla_k^2 = \sum_k \mathbf{h}^{(k)} \quad (2.16)$$

and

$$\mathbf{H}_2 = \frac{1}{2} \sum_{k \neq l} \frac{e^2}{|\vec{r}_k - \vec{r}_l|} = \frac{1}{2} \sum_{k \neq l} \mathbf{w}^{(kl)}. \quad (2.17)$$

The total energy of the system can be written as

$$E = E[\tilde{\psi}] = \langle \tilde{\psi} | \mathbf{H} | \tilde{\psi} \rangle = \langle \tilde{\psi} | \mathbf{H}_1 | \tilde{\psi} \rangle + \langle \tilde{\psi} | \mathbf{H}_2 | \tilde{\psi} \rangle \quad (2.18)$$

where  $|\tilde{\psi}\rangle$  is a eigenfunction constituted from tensor products of Z arbitrary kets  $|\alpha^1\rangle, |\beta^2\rangle, \dots$

$$\begin{aligned} |\tilde{\psi}\rangle &= |\alpha^1\rangle |\beta^2\rangle \dots |\lambda^k\rangle \dots |\zeta^z\rangle \\ &= |\alpha^1 \beta^2 \dots \lambda^k \dots \zeta^z\rangle \end{aligned} \quad (2.19)$$

where  $a, b, c, \dots, \lambda, \dots, \zeta$  represent the states of one-electron states, and  $(1), (2), \dots, (k), \dots, (Z)$  represent coordinate of an individual electron with an orthonormalized constraint

$$\langle \lambda | \mu \rangle = \delta_{\lambda\mu} \quad \text{where } \lambda, \mu = \alpha, \beta, \dots, \zeta.$$

The expectation value of  $\mathbf{H}_1$  becomes successively

$$\begin{aligned} \langle \mathbf{H}_1 \rangle &= \langle \tilde{\psi} | \mathbf{H}_1 | \tilde{\psi} \rangle = \left\langle \tilde{\psi} \left| \sum_k \mathbf{h}^{(k)} \right| \tilde{\psi} \right\rangle \\ &= \sum_k \langle \tilde{\psi} | \mathbf{h}^{(k)} | \tilde{\psi} \rangle \\ &= \sum_{\lambda} \langle \lambda | \mathbf{h}^{(1)} | \lambda \rangle \end{aligned} \quad (2.20)$$

and

$$\begin{aligned} \langle \mathbf{H}_2 \rangle &= \langle \tilde{\psi} | \mathbf{H}_2 | \tilde{\psi} \rangle = \left\langle \tilde{\psi} \left| \frac{1}{2} \sum_{k \neq l} \mathbf{w}^{(kl)} \right| \tilde{\psi} \right\rangle \\ &= \frac{1}{2} \sum_{k \neq l} \langle \tilde{\psi} | \mathbf{w}^{(kl)} | \tilde{\psi} \rangle \\ &= \frac{1}{2} \sum_{\lambda \neq \mu} \langle \lambda^{(1)} \mu^{(2)} | \mathbf{w}^{(12)} | \lambda^{(1)} \mu^{(2)} \rangle. \end{aligned} \quad (2.21)$$

According to the variational technique, we seek to minimize with respect to variations in the single-electron wavefunctions,  $|\lambda\rangle$ . At the same time, the wavefunctions are constrained to be orthonormal,  $\langle \lambda | \mu \rangle = \delta_{\lambda\mu}$ . Therefore we use the method of Lagrange multipliers:

$$\delta \left\{ E[\tilde{\psi}] + \sum_{\lambda\mu} \varepsilon_{\lambda\mu} \langle \lambda | \mu \rangle \right\} = 0, \quad (2.22)$$

where  $\delta$  is a variation with respect to any of the single-electron wavefunctions. Using linear combinations of  $|\alpha\rangle, |\beta\rangle, \dots, |\zeta\rangle$  that diagonalize  $\varepsilon_{\lambda\mu}$ , one get

$$\delta E[\tilde{\psi}] + \sum_{\lambda} \varepsilon_{\lambda} \delta \langle \lambda | \lambda \rangle = 0. \quad (2.23)$$

This can be developed to

$$\begin{aligned} & \sum_{\lambda} \langle \delta\lambda | \left\{ \mathbf{h}^{(1)} | \lambda^{(1)} \rangle + \sum_{\mu} \langle \mu^{(2)} | \mathbf{w}^{(12)} | \mu^{(2)} \rangle | \lambda^{(1)} \rangle - \varepsilon_{\lambda} | \lambda \rangle \right\} \\ & + \sum_{\lambda} \left\{ \langle \lambda^{(1)} | \mathbf{h}^{(1)} + \sum_{\mu} \langle \lambda^{(1)} | \langle \mu^{(2)} | \mathbf{w}^{(12)} | \mu^{(2)} \rangle - \varepsilon_{\lambda} \langle \lambda | \right\} | \delta\lambda \rangle = 0 \end{aligned} \quad (2.24)$$

it is clearly seen that whole left side of equation can be zero if

$$\mathbf{h}^{(1)} | \lambda^{(1)} \rangle + \sum_{\mu} \langle \mu^{(2)} | \mathbf{w}^{(12)} | \mu^{(2)} \rangle | \lambda^{(1)} \rangle - \varepsilon_{\lambda} | \lambda \rangle = 0 \quad (2.25)$$

This equation is called the Hartree equation.

### Hartree-Fock Equation

The Hartree equation was derived based on the assumption that  $|\tilde{\psi}\rangle$  is a tensor product of  $Z$  arbitrary kets,  $|\alpha^{(1)}\rangle, |\beta^{(2)}\rangle, \dots$ , which can give a good approximation for some systems. However, the Hartree equation itself does not include the effect of Pauli's exclusion principle, which requires the electron wave function to be antisymmetric under particle interchanges. The wave function now becomes

$$|\psi\rangle = (Z!)^{-1/2} \sum_P (-1)^P \mathbf{P} |\tilde{\psi}\rangle = (Z!)^{-1/2} \mathbf{A} |\tilde{\psi}\rangle \quad (2.26)$$

where  $\mathbf{P}$  is permutation operators, and  $\mathbf{A}$  is the antisymmetric operator defined by

$$\mathbf{A} = \frac{1}{Z!} \sum_P (-1)^P \mathbf{P} \quad (2.27)$$

Then we apply the variational method with  $|\psi\rangle$  in the same way as did with  $|\tilde{\psi}\rangle$  yields

$$\langle \mathbf{H}_1 \rangle = \sum_{\lambda} \langle \lambda | \mathbf{h}^{(1)} | \lambda \rangle \quad (2.28)$$

and

$$\langle \mathbf{H}_2 \rangle = \frac{1}{2} \sum_{\lambda\mu} \langle \lambda^{(1)} \mu^{(2)} | \mathbf{w}^{(12)} | \lambda^{(1)} \mu^{(2)} \rangle - \langle \lambda^{(1)} \mu^{(2)} | \mathbf{w}^{(12)} | \mu^{(1)} \lambda^{(2)} \rangle, \quad (2.29)$$

where the first term of  $\langle \mathbf{H}_2 \rangle$  is the Coulomb interaction term, and the second term is the exchange interaction term. Then we can obtain

$$\mathbf{h}^{(1)} | \lambda^{(1)} \rangle + \sum_{\mu} \langle \mu^{(2)} | \mathbf{w}^{(12)} | \mu^{(2)} \rangle | \lambda^{(1)} \rangle - \sum_{\mu} \langle \mu^{(2)} | \mathbf{w}^{(12)} | \lambda^{(2)} \rangle | \mu^{(1)} \rangle - \varepsilon_{\lambda} | \lambda \rangle = 0$$

$$\text{or} \quad \mathbf{F} | \lambda \rangle - \varepsilon_{\lambda} | \lambda \rangle = 0 \quad (2.30)$$

which is called the Hartree-Fock equation,

where the Fock operator  $\mathbf{F}$  is defined as

$$\mathbf{F} | \lambda \rangle = \mathbf{h} | \lambda \rangle + \sum_{\mu} \langle \mu^{(2)} | \mathbf{w}^{(12)} | \mu^{(2)} \rangle | \lambda^{(1)} \rangle + \sum_{\mu} \langle \mu^{(2)} | \mathbf{w}^{(12)} | \lambda^{(2)} \rangle | \mu^{(1)} \rangle \quad (2.31)$$

Some more approximations must be introduced in order to solve the Hartree-Fock equation. The wave function,  $| \lambda \rangle$ , can be written as a linear combination of basis function.

$$| \lambda \rangle = \sum_j c_{\lambda j} | j \rangle \quad (2.32)$$

substituting this into Hartree-Fock equation and multiply by  $\langle i |$  we obtain the result

$$\sum_j c_{\lambda j} \langle i | \mathbf{F} | j \rangle = \varepsilon_{\lambda} \sum_j c_{\lambda j} \langle i | j \rangle. \quad (2.33)$$

It can be rewritten in form of matrix equation

$$\sum_j c_{\lambda j} (F_{ij} - \varepsilon_{\lambda} S_{ij}) = 0 \quad (2.34)$$

where  $F_{ij} = \langle \phi_i | \mathbf{F} | \phi_j \rangle$  are elements of the Fock matrix  $\mathbf{F}$ , and  $S_{ij} = \langle \phi_i | \phi_j \rangle$  are elements of the overlap matrix  $\mathbf{S}$ . The equation can be rewritten in the more compact matrix form

$$\mathbf{F} \mathbf{c} = \mathbf{S} \mathbf{c} \varepsilon. \quad (2.35)$$



This equation is called the Roothaan-Hall equation, which provides the ability to solve the Hartree-Fock equation with numerical procedures using digital computers [Roothaan, 1951; Hall, 1951]. This technique is commonly used in problem solving and is called the Roothaan Hartree-Fock Self Consistent Field method (SCF).

## 2.7 Basis set superposition error

In the calculation of stabilization energies, using the SCF method, of two species, A and B, an erroneous result is obtained when finite bases are employed. The reason is the finite separation of two species sites of A and B. The basis set located on B sites can overlap and improve the basis set of A, and vice versa. To estimate the effect, the energy of the A species is calculated with both basis sets of A and B, but without the B species itself. Next, one calculates for the B species with both basis sets of A and B, without the A species. The results can be used to improve the value of the total energy. The Counterpoise method was first introduced by Boys and Bernardi [1970] to correct the inaccuracy. This method determines the subsystem energies using the same basis set functions as used in the full system. Suppose that  $\{A\}$  and  $\{B\}$  are the basis sets of subsystems A and B, respectively. The interaction energy of whole system can be written as

$$\Delta E = E_{AB}(\{A\}, \{B\}) - (E_A(\{A\}) + E_B(\{B\})) \quad (2.36)$$

and the Counterpoise correction as

$$\Delta e = (E_A(\{A\}) - E_A(\{A\}, \{B\})) + (E_B(\{B\}) - E_B(\{A\}, \{B\})) \quad (2.37)$$

The Counterpoise corrected interaction energy can be written

$$\Delta E_{c.p.} = \Delta E + \Delta e. \quad (2.38)$$

# CHAPTER 3

## MOLECULAR DYNAMICS SIMULATION

### 3.1 What is Molecular Dynamics?

Molecular dynamics (MD) is a computer simulation technique where the time evolution of a set of interacting atoms is followed by integrating their equations of motion. In molecular dynamics one follows the laws of classical mechanics, and most notably Newton's law:

$$F_i = m_i a_i \quad (3.1)$$

for each atom  $i$  in a system constituted by  $N$  atoms. Here,  $m_i$  is the atomic mass,  $a_i = d^2 r_i / dt^2$  its acceleration, and  $F_i$  the force acting upon it, due to the interactions with other atoms. Therefore, in contrast with the Monte Carlo method, molecular dynamics is a deterministic technique: given an initial set of positions and velocities, the subsequent time evolution is in principle completely determined. In more pictorial terms, atoms will "move" into the computer, bumping into each other, wandering around (if the system is fluid), oscillating in waves in concert with their neighbors, perhaps evaporating away from the system if there is a free surface, and so on, in a way pretty similar to what atoms in a real substance would do.

The computer calculates a trajectory in a  $6N$ -dimensional phase space ( $3N$  positions and  $3N$  momenta). However, such trajectory is usually not particularly relevant by itself. *Molecular dynamics is a statistical mechanics method.* Like Monte Carlo, it is a way to obtain a set of configurations distributed according to some statistical distribution function, or statistical ensemble. An example is the microcanonical ensemble, corresponding to a probability density in phase space

where the total energy is a constant  $E$ :  $\delta(H(\Gamma) - E)$ . Here,  $H(\Gamma)$  is the Hamiltonian, and represents the set of positions and momenta.  $\delta$  is the Dirac function, selecting out only those states which have a specific energy  $E$ . Another example is the canonical ensemble, where the temperature  $T$  is constant and the probability density is the Boltzmann function  $\exp(-H(\Gamma)/k_{\text{B}}T)$

According to statistical physics, physical quantities are represented by averages over configurations distributed according to a certain statistical ensemble. A trajectory obtained by molecular dynamics provides such a set of configurations. Therefore, a measurement of a physical quantity by simulation is simply obtained as an arithmetic average of the various instantaneous values assumed by that quantity during the MD run. Statistical physics is the link between the microscopic behavior and thermodynamics. In the limit of very long simulation times, one could expect the phase space to be fully sampled, and in that limit this averaging process would yield the thermodynamic properties. In practice, the runs are always of finite length, and one should exert caution to estimate when the sampling may be good (system at equilibrium) or not. In this way, MD simulations can be used to measure thermodynamic properties and therefore evaluate, say, the phase diagram of a specific material.

### 3.2 Historical Molecular Dynamics

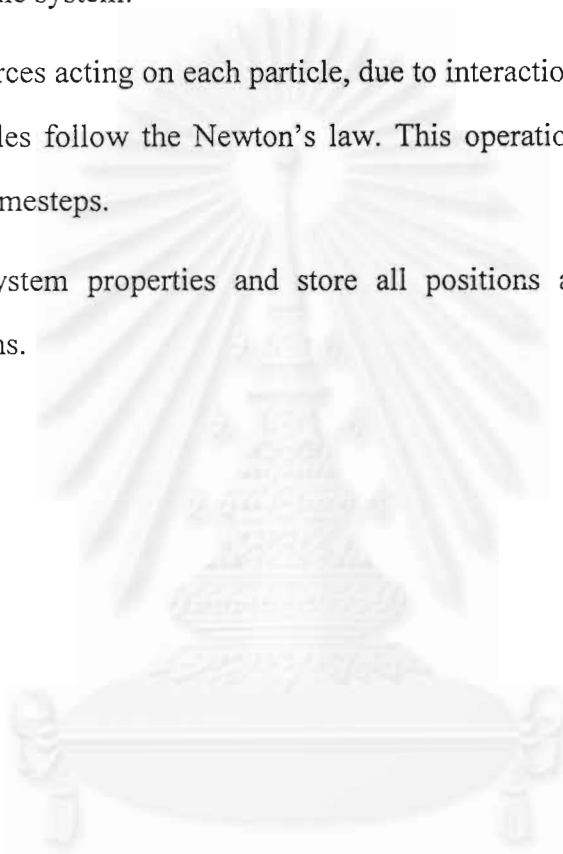
- The first paper reporting a molecular dynamics simulation was written by Alder and Wainwright [1957]. The purpose of the paper was to investigate the phase diagram of a hard sphere system, and in particular the solid and liquid regions. In a hard sphere system, particles interact via instantaneous collisions, and travel as free particles between collisions. The calculations were performed on a UNIVAC and on an IBM 704.

- The article *Dynamics of radiation damage* by Gibson, Goland, Milgram and Vineyard from Brookhaven National Laboratory, appeared in 1960, is probably the first example of a molecular dynamics calculation with a continuous potential based on a finite difference time integration method. The calculation for a 500-atoms system was performed on an IBM 704, and took about a minute per time step. The paper, dealing with creation of defects induced by radiation damage (a theme appropriate to *cold war* days), is done exceedingly well, and is hard to believe that it is almost 40 years old.
- Rahman at Argonne National Laboratory has been a well known pioneer of molecular dynamics. In this famous 1964 paper *Correlations in the motion of atoms in liquid argon*, he studies a number of properties of liquid Ar, using the Lennard-Jones potential on a system containing 864 atoms and a CDC 3600 computer. The legacy of Rahman's computer codes is still carried by many molecular dynamics programs in operation around the world, descendant of Rahman's.
- Verlet calculated in 1967 the phase diagram of argon using the Lennard-Jones potential, and computed correlation functions to test theories of the liquid state. The bookkeeping device which became known as *Verlet neighbor list* was introduced in these papers. Moreover the "Verlet time integration algorithm" was used. Phase transitions in the same system were investigated by Hansen and Verlet a couple of years later.

### 3.3 Molecular Dynamics Procedure

To perform molecular dynamics simulation it may be possible to consider the following steps (Figure 3.1):

- Prepare necessary constants and initialize coordinations and velocities of all particles in the system.
- Calculate forces acting on each particle, due to interactions with its neighbors, and move particles follow the Newton's law. This operation is repeated for a large number of timesteps.
- Calculate system properties and store all positions and velocities for future investigations.



จุฬาลงกรณ์มหาวิทยาลัย

## The Scheme in Molecular Dynamics Simulation

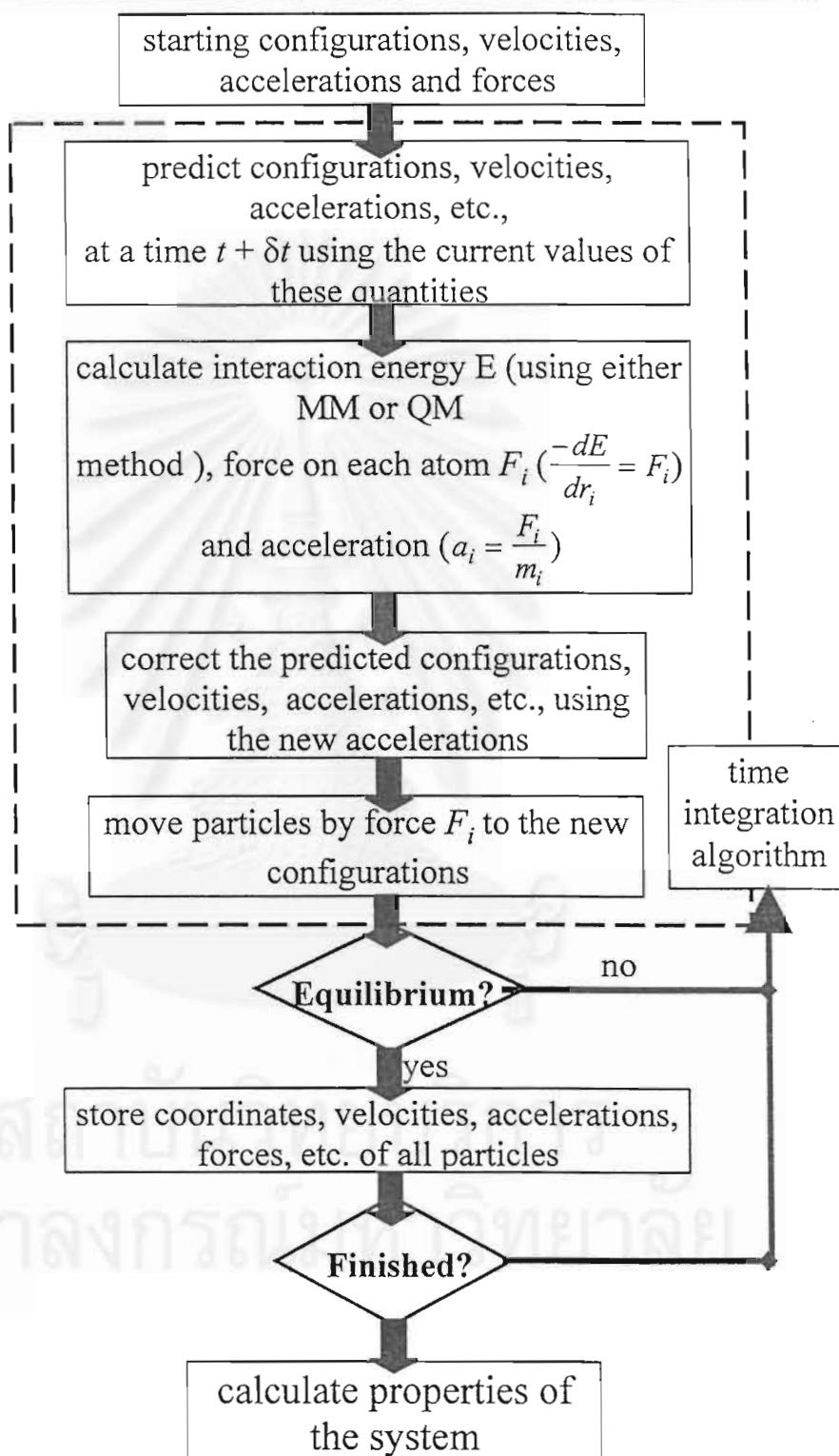


Figure 3.1 Scheme in molecular dynamics simulation (MM and QM denote Molecular Mechanics and Quantum Mechanics, respectively).

### 3.3.1 The Predictor-Corrector Algorithm

The finite difference approach is a standard method for solving systems of differential equations. A basic concept, called the predictor-corrector algorithm, supposes that one knows the positions, velocities, etc. at time  $t$ . Then one can estimate positions, velocities, etc. at time  $t + \delta t$  from a Taylor series expansion around  $t$

$$\begin{aligned}
 \bar{r}^p(t + \delta t) &= \bar{r}(t) + \delta t \bar{v}(t) + \frac{1}{2} \delta t^2 \bar{a}(t) + \frac{1}{6} \delta t^3 \bar{b}(t) + \dots \\
 \bar{v}^p(t + \delta t) &= \bar{v}(t) + \delta t \bar{a}(t) + \frac{1}{2} \delta t^2 \bar{b}(t) + \dots \\
 \bar{a}^p(t + \delta t) &= \bar{a}(t) + \delta t \bar{b}(t) + \dots \\
 \bar{b}^p(t + \delta t) &= \bar{b}(t) + \dots,
 \end{aligned} \tag{3.3}$$

where  $\bar{r}(t)$ ,  $\bar{v}(t)$ ,  $\bar{a}(t)$ , and  $\bar{b}(t)$  represent positions, velocities, accelerations and the first derivative of accelerations, respectively, at time  $t$ . The superscript  $p$  marks a *predicted* value. However, in the present step, these formulas cannot generate sufficiently precise trajectories as time evolves because the value of  $\bar{b}(t)$  is not given yet and is thus initially set to zero. One way to improve the result is to determine  $\bar{b}(t)$  from  $\bar{a}(t)$  and  $\bar{a}(t + \delta t)$  using

$$\bar{b}(t) \approx \frac{\bar{a}(t + \delta t) - \bar{a}(t)}{\delta t}. \tag{3.4}$$

In the next step, the corrector step, the new  $\bar{b}(t)$  is used to recalculate the new set of  $\bar{r}(t + \delta t)$ ,  $\bar{v}(t + \delta t)$ ,  $\bar{a}(t + \delta t)$ , and  $\bar{b}(t + \delta t)$  using equation (3.3). The corrector step may be iterated. Nevertheless, in our simulations only one corrector step was performed.

Another way to obtain a better trajectory is the method introduced by Gear [1966; 1971]. The corrected accelerations,  $\bar{a}^c(t + \delta t)$ , at predicted positions,  $\bar{r}^p(t + \delta t)$ , are calculated and brought to compare with predicted accelerations,  $\bar{a}^p(t + \delta t)$ , yielding the estimated size of the error in the prediction step:

$$\Delta \bar{a}(t + \delta t) = \bar{a}^c(t + \delta t) - \bar{a}^p(t + \delta t). \tag{3.5}$$

The error size and results from the predictor step are used in the correction step, e.g.,  
by

$$\begin{aligned}
 \bar{r}^c(t + \delta t) &= \bar{r}^p(t + \delta t) + c_0 \Delta \bar{a}(t + \delta t) \\
 \bar{v}^c(t + \delta t) &= \bar{v}^p(t + \delta t) + c_1 \Delta \bar{a}(t + \delta t) \\
 \bar{a}^c(t + \delta t) &= \bar{a}^p(t + \delta t) + c_2 \Delta \bar{a}(t + \delta t) \\
 \bar{b}^c(t + \delta t) &= \bar{b}^p(t + \delta t) + c_3 \Delta \bar{a}(t + \delta t).
 \end{aligned}
 \tag{3.6}$$

The values of corrector coefficients depend on the choice of process used in the calculation, such as the order of finite difference being used in the algorithm.

### 3.3.2 Periodic Boundary Conditions

The number of particles in computer simulations is usually limited by the efficiency of the computer. Only a few thousand particles, compared to  $6 \times 10^{23}$  per mole of a real system, can be simulated in a tiny container. It can be supposed that a large fraction of particles lies near the container walls. Those particles will experience quite different interactions from particles in the bulk. Nevertheless, this problem can be overcome by introducing periodic boundary conditions to simulate infinite systems [Born and Karman, 1912]. The container, usually of cubic shape, is replicated throughout space to form an infinite lattice. The particles in the original container and its periodic images will progress in the same way in the course of simulations. When a particle leaves the container by crossing a boundary, there will be an image of that particle entering the container on the opposite boundary.



### 3.3.3 Cut-Off Limit

In the case of short-range interactions, rapidly dropping to zero, one can neglect the interactions beyond a distance called the cut-off limit. Normally, it is never greater than half of the periodic box-length to include only the nearest images of distinguishable particles in interaction calculations.

### 3.3.4 Long-Range Interactions

Interactions over distances far beyond half of the periodic box length are called long-range interactions. Sometimes they cannot be ignored, and they make computer simulations more difficult. Two standard techniques for this problem are Ewald summation [Ewald, 1921] and reaction field correction [Onsager, 1936].

The Ewald summations handle all particles with their images as they are in a solid crystallized system. In case of coulombic interaction the potential energy of the system,  $V$ , can be written down as

$$V = \frac{1}{2} \sum_{\vec{n}} \left( \sum_{i,j} Z_i Z_j \frac{1}{|\vec{r}_{ij} + \vec{n}L|} \right), \quad (3.7)$$

where  $i, j$  represent all particles in the periodic box, and  $\vec{n}$  is a vector of integers representing the periodic images. This summation conditionally converges to a known limit for numerous sorts of long-range potentials.

The reaction field method introduced without the assumption of periodicity, treats all particles beyond the cut-off sphere as forming a continuum with a given dielectric constant. Therefore, any charge lying inside the cut-off sphere will polarize the continuum and create a reaction field at the center.

### 3.3.5 Shifted and Shifted-Force Potentials

The truncation of the potential at a cut-off introduces some difficulties in defining a consistent potential and force, since the potential function,  $V(r_{ij})$ , contains a discontinuity at  $r_{ij} = r_{cutoff}$ . The problem may be avoided by shifting the potential function by an amount  $V_c = V(r_c)$ . However, the force at  $r_{ij} = r_{cutoff}$  is still discontinuous. For conservation of energy, the shift-force potential method [Streett, 1978] is introduced, and the shift-force potential can be calculated from equation (3.8).

$$V_{shift-force}(r_{ij}) = \begin{cases} V(r_{ij}) - V_c - V'(r_c)(r_{ij} - r_c) & r_{ij} \leq r_c \\ 0 & r_{ij} > r_c \end{cases} \quad (3.8)$$

## 3.4 Calculation of Macroscopic Properties

### 3.4.1 Structural Properties

Liquid structure cannot be written as an exact arrangement in space as in the case of crystalline solids. It is usually be described in terms of comparative arrangements of atoms with other atoms. One essential measure is the radial

distribution function (RDF), represented by  $g_{ij}(r)$ . This function presents the probability per unit volume of finding particle  $j$  at distance  $r$  from particle  $i$ . The RDF is normalized to be 1 for a completely random distribution. Another quantity related to the RDF is the running integration number, represented by  $n_{ij}(r)$ , easily calculated from

$$n_{ij}(r) = \rho \int_0^r g_{ij}(r) 4\pi r^2 dr, \quad (3.9)$$

where

$$\rho = \text{number density} = N/V.$$

An average coordination number is defined as the value of  $n_{ij}(r)$  at the first minimum of  $g_{ij}(r)$  following the first peak. Any particles at distances less than this first minimum belong to the first solvation shell.

### 3.4.2 Dynamical Properties

The most common way to present dynamical properties of the system is to formulate via the time-correlation function,

$$C_{AB}(t) = \frac{\langle A(0)B(t) \rangle}{\langle A(0)B(0) \rangle} \quad (3.10)$$

where  $\langle A(0)B(t) \rangle$  can be calculated using the averaging formula,

$$\langle A(0)B(t) \rangle = \frac{1}{t_{\max}} \sum_{t_0=1}^{t_{\max}} A(t_0)B(t_0+t). \quad (3.11)$$

Another meaningful dynamical property is the time-autocorrelation function, defined as

$$C_{AA}(t) = \langle A(0)A(t) \rangle, \quad (3.12)$$

and yet another is the self-diffusion coefficient,  $D$ , which is related to the velocity autocorrelation function by the Green-Kubo relation [Frenkel and Smit 1996],

$$D = \frac{1}{3} \int C_{vv}(t) dt \quad (3.13)$$

The elementary Stokes-Einstein theory of diffusion of liquid [Frenkel 1946] shows that the relation of the self-diffusion coefficient,  $D$ , and viscosity,  $\nu$ , is

$$D = \frac{1}{6\pi a} \frac{k_B T}{\nu}, \quad (3.14)$$

where  $a$  is the radius of fluid particle,  $k_B$  is Boltzmann's constant, and  $T$  is the absolute temperature.



จุฬาลงกรณ์มหาวิทยาลัย

## CHAPTER 4

### DETAIL OF CALCULATIONS

Lithium-liquid ammonia solution consists of ammonia molecules, lithium ions and free (conduction) electrons. In this study two different models of the pseudopotential have been employed. The molecular dynamics simulation has been used to calculate structural and dynamical properties of highest concentrated lithium-ammonia solutions.

#### 4.1 Simulation Models

##### 4.1.1 Total Energy

The total potential which describes the effective interaction for all particles in the flexible MD simulations consists of 2 parts namely inter- and intramolecular potential functions, Interaction between sites of kind  $i$  and  $j$  in metal ammonia system containing free electrons is given by

$$V^{ij}(\mathbf{R}) = V^{ij}_{\text{dir}}(\mathbf{R}) + V^{ij}_{\text{ind}}(\mathbf{R}) \quad (4.1)$$

where  $V^{ij}_{\text{dir}}(\mathbf{R})$  is the direct interaction and  $V^{ij}_{\text{ind}}(\mathbf{R})$  is the change of the direct interaction due to the presence of free electrons.

The  $V^{ij}_{\text{dir}}(\mathbf{R})$  is usually developed using quantum chemical calculations while the  $V^{ij}_{\text{ind}}(\mathbf{R})$  can be calculated using pseudopotential method [Hannongbua et al. 1988, 1992, 1997]

In this chapter, three types of the functions,  $V_{\text{intra}}$ ,  $V^{ij}_{\text{dir}}(\mathbf{R})$  and  $V^{ij}_{\text{ind}}(\mathbf{R})$  have been described.

### 4.1.2 Ammonia Intramolecular Potential

Several intramolecular potential describing flexibility of the ammonia molecule available in the literatures [Bopp et al. 1982, 1984, Spirko 1983]. They are derived base on spectroscopic data. In this study that reported by Spirko has been used. This function accounts also for the inversion mode of the molecule by means of a strongly anharmonic potential. The potential function is given by,

$$\begin{aligned}
 V_{intra} = & \sum_{i=1}^4 k_i h^{2i} + k'_1 h^2 s_1 + k'_2 h^4 s_1 \\
 & + \frac{1}{2} \sum_{i=1}^5 \sum_{j=i}^5 F_{ij} s_i s_j + \sum_{i=1}^5 \sum_{j=i}^5 \sum_{k=j}^5 F_{ijk} s_i s_j s_k \\
 & + \sum_{i=1}^5 \sum_{j=i}^5 \sum_{k=j}^5 \sum_{l=k}^5 F_{ijkl} s_i s_j s_k s_l.
 \end{aligned} \tag{4.2}$$

The symmetry coordinates  $s_i$  are defined as

$$\begin{aligned}
 s_1 &= \frac{1}{\sqrt{3}} (\Delta r_1 + \Delta r_2 + \Delta r_3), \\
 s_2 &= \frac{1}{\sqrt{6}} (2\Delta r_1 - \Delta r_2 - \Delta r_3), \\
 s_3 &= \frac{1}{\sqrt{6}} (2\Delta \alpha_1 - \Delta \alpha_2 - \Delta \alpha_3), \\
 s_4 &= \frac{1}{\sqrt{2}} (\Delta r_2 - \Delta r_3), \\
 s_5 &= \frac{1}{\sqrt{2}} (\Delta \alpha_2 - \Delta \alpha_3),
 \end{aligned} \tag{4.3}$$

where  $\Delta r_i$  and  $\Delta \alpha_i$  are the three N-H distances and H-N-H angles, respectively.  $h$  is the distance of the nitrogen atom from the plan spanned by the three hydrogen atoms, and all constants are given by

Inversion force constants,

$k_1$	$= -0.53741$	$k'_1$	$= +1.0806$
$k_2$	$= +2.08241$	$k'_2$	$= -5.7569$
$k_3$	$= -0.77902$		
$k_4$	$= +0.3500$		

Second-order force constants,

$$\begin{aligned}
 F_{11} &= 6.8186 \\
 F_{12} &= F_{44} = 6.8975 \\
 F_{33} &= F_{55} = 0.6166 \\
 F_{23} &= F_{45} = 0.0028
 \end{aligned}$$

Third-order force constants,

$$\begin{aligned}
 F_{111} &= -3.92836 \\
 F_{122} &= F_{144} = -11.9988 \\
 F_{123} &= F_{145} = -4.8718 \times 10^{-3} \\
 F_{133} &= F_{155} = -0.10989 \\
 F_{222} &= -2.82914 \\
 F_{244} &= 8.4874 \\
 F_{223} &= -F_{344} = 5.9505 \times 10^{-6} \\
 F_{245} &= 1.1901 \times 10^{-5} \\
 F_{233} &= -F_{255} = -1.0983 \times 10^{-3} \\
 F_{345} &= 21.966 \times 10^{-3} \\
 F_{333} &= -0.06747 \\
 F_{355} &= 0.2024
 \end{aligned}$$

Fourth-order force constants,

$$\begin{aligned}
 F_{1111} &= 2.8351 \\
 F_{1122} &= F_{1144} = 17.163 \\
 F_{1133} &= F_{1155} = 0.08564 \\
 F_{1222} &= 8.1277 \\
 F_{1244} &= -24.3830 \\
 F_{1333} &= 0.01625 \\
 F_{1355} &= -0.04875 \\
 F_{2222} &= F_{4444} = 4.3066 \\
 F_{2244} &= 8.6133 \\
 F_{2233} &= F_{2255} = F_{3344} \\
 &= F_{4455} = 0.04078 \\
 F_{3333} &= F_{5555} = 0.08044 \\
 F_{3355} &= 0.16087
 \end{aligned}$$

For this model of intramolecular potential is well known for flexible molecule ammonia in molecular dynamics simulation.

### 4.1.3 Intermolecular Potentials

The interactions between particles in the system are described by potential function which varies according to the characteristics of components, such as the electromagnetic force, overlap, induction, etc. However, the potential of any system can be written, in general form, as

$$U(\vec{r}_1, \vec{r}_2, \dots, \vec{r}_n) = \sum_{i=1}^n U(\vec{r}_i) + \sum_{i=1}^n \sum_{j=i+1}^n U(\vec{r}_i, \vec{r}_j) + \sum_{i=1}^n \sum_{j=i+1}^n \sum_{k=j+1}^n U(\vec{r}_i, \vec{r}_j, \vec{r}_k) + \dots \quad (4.4)$$

The first term of the right side of equation,  $U_1(\vec{r}_i)$ , represents the influence from a potential due to the external force field, such as the gravity field. The second function,  $U_2(\vec{r}_i, \vec{r}_j)$ , called the pair potential, represents the potential from two body interactions. It is usually the most important term and can be written as a function of the magnitude of the distance between the pairs. The next term,  $U_3(\vec{r}_i, \vec{r}_j, \vec{r}_k)$ , called the three-body term, is generally expected to be small and is neglected in a number of models because it slows down computer simulations as well as requiring much time and effort for the development of the function. However, in the case of condensed systems, the three-body term probably becomes meaningful and affects some outrun properties. The remaining terms, called non-additive or many-body interaction terms, are generally expected to have very small effects on the system.

#### Pair Potential

Concentrated lithium–ammonia solution is a quantum system which consisting of lithium ions and free electrons in liquid ammonia, the system has to be described by the pair potential and pseudopotential. The last one is necessary to describe the effect of the free electrons on the pair potentials which are routinely used for classical simulations.



In this study, ammonia-ammonia potential function and parameter parameters (Table 4.1), were taken from [Hannongbua, et al., 1988]. The lithium-lithium and lithium-ammonia potential function and parameter (Table 4.2) [Hannongbua, et al., 1992] have been applied

Table 1. Directed intermolecular potentials employed in simulation. Energies are given in units of  $10^{-19}$  J with the distances in Å.

$$\begin{aligned} V_{NN}(R) &= 14.85/R + 55719/R^{12} - 13.6/R^6 \\ V_{NH}(R) &= -4.95/R + 0.01042\{\exp[-4.6(R-2.4)]-2\exp[-2.3(R-2.4)]\} \\ V_{HH}(R) &= 165/R + 48.64\exp(-3.7R) \end{aligned}$$

Table 4.2 Parameter potential functions for the Li-ammonia pair potentials function the energy are given in  $\text{kJ mol}^{-1}$  with R in Å.

$V^{ij}(R) = \frac{A}{R} + \frac{B}{R^6} + C \exp(-DR)$				
	A	B	C	D
Li-Li	1390	0	-18.7	1.62
Li-N	-1686	4024	0	-
Li-H	562	2865	-229	0.31

### Pseudopotential

In comparison to the previous studies [Hannongbua et al. 1988, 1992, 1997]. The effective volume,  $\Omega_E$  is newly defined. Total volume of the simulation cube ( $\Omega$ ) is substituted by those occupied by metal ions ( $\Omega_m$ ) and by ammonia volume ( $\Omega_a$ ). According to the Pauli's exclusion principle, i.e.,

$$\Omega_E = \Omega - N_m\Omega_m - N_a\Omega_a, \quad (4.5)$$

where  $N_m$  and are numbers of lithium atoms and ammonia molecules, respectively.

Volumes of  $N_m$  metal ions and  $N_a$  ammonia molecules were calculated by,

$$\Omega_m = \frac{4\pi}{3} r_{c,m}^3 \text{ and } \Omega_a = \frac{4\pi}{3} r_a^3 \quad (4.6)$$

$r_{c,m}$  and  $r_a$  are effective radius of lithium ions ( $r_{c,m}=1.28$ ) and ammonia molecules ( $r_a = 4.3$ ) [Hannongbua, et al., 1992] A set of model pseudopotential which is used to represent the electron-site interactions has the form of Ashcroft's Model Pseudopotential [1966]:

$$w_{e-H}(q) = -\frac{4\pi Z_H}{\Omega_E q^2}$$

$$w_{e-j}(q) = -\frac{4\pi Z_j}{\Omega_E q^2} \cos(qr_{c,j})$$

with  $j = N, Li$ ;  $r_{c,N} = 1.51$  and  $Z_N = -0.8022$ ,  $Z_H = 0.2674$ ,  $Z_{Li} = 1$ .

Atomic units are used in all equations throughout this study. Notation  $w_i(q)$  and  $\varepsilon(q)$  are the form factor and the dielectric function will define below. By the use of pseudopotential theory and assumption that electron states from a spherical Fermi surface, one obtains,

$$V_{ind}^{ij}(R) = \frac{\Omega_E}{\pi^2} \int_0^\infty F(q) \frac{\sin qR}{R} q dq, \quad (4.7)$$

when,

$$F_{ij}(q) = \frac{\Omega_E q^2}{8\pi} w_i(q) \frac{1 - \varepsilon(q)}{\varepsilon(q)} w_j(q), \quad (4.8)$$

and

$$\varepsilon(q) = 1 + \frac{4\pi}{q^2} \Pi(q) \quad (4.9)$$

$$\Pi(q) = \frac{k_F}{\pi^2} \frac{f(x)}{1 - (4\mu^2/x^2)G(x)f(x)} \quad (4.10)$$

$$x = \frac{q}{k_F}, \quad \mu^2 = \frac{1}{\pi k_F}, \quad k_F = \left( \frac{3\pi^2 Z_m N_m}{\Omega - N_m \Omega_m - N_a \Omega_a} \right)^{1/3} \quad (4.11)$$

and

$$f(x) = \frac{1}{2} + \frac{4-x^2}{8x} \ln \left| \frac{2+x}{2-x} \right| \quad (4.12)$$

Two models of the local field function are employed in this work.

**Model I.** Geldart-Vosko local field function [Gurskii 1992]

$$G(x) = \frac{1}{2} \frac{x^2}{x^2 + 2(1 + 0.153\mu^2)^{-1}} \quad (4.13)$$

**Model II.** Ichimaru's local field function [Ichimaru and Usumi, 1981].

$$G(x) = Ax^4 + Bx^2 + C + \left( Ax^4 + \left( B + \frac{8}{3}A \right) x^2 - C \right) \left( \frac{4-x^2}{4x} \ln \left| \frac{2+x}{2-x} \right| \right) \quad (4.14)$$

when

$$A = 0.029$$

$$B = \frac{2}{16} \gamma_0(r_S) - \frac{3}{64} [1 - g(0)] - \frac{16}{15} A$$

$$C = -\frac{3}{4} \gamma_0(r_S) + \frac{2}{16} [1 - g(0)] - \frac{16}{5} A$$

$$g(0) = \frac{1}{8} \left( \frac{Z}{I_1(Z)} \right)^2 \quad I_1(Z) = \text{modified Bessel function.}$$

$$Z = 4 \left( \frac{\lambda r_S}{\pi} \right)^{1/2}, \quad \lambda = \left( \frac{4}{9\pi} \right)^{1/3}, \quad r_S = \frac{1}{\lambda k_F}$$

$$\gamma_0(r_S) = \frac{1}{4} + \frac{\frac{\lambda\pi}{8} d_0 y_2 \left[ 1 + 2d_1 y_1 + \left( \frac{4}{3} d_2 + d_1^2 \right) y_2 + \left( \frac{3}{2} d_3 + \frac{7}{6} d_1 d_2 \right) y_3 + \frac{4}{3} d_1 d_3 y_2^2 \right]}{\left[ 1 + d_1 y_1 + d_2 y_2 + d_3 y_3 \right]^2}$$

$$d_0 = 0.06218 \quad d_2 = 2.82224$$

$$d_1 = 9.81379 \quad d_3 = 0.73641$$

where

$$y_1 = r_S^{1/2}, \quad y_2 = r_S, \quad y_3 = r_S^{3/2}$$

## 4.2 Molecular Dynamics Simulation

In this study, molecular dynamics simulations of the lithium-ammonia solution have been performed for the concentrated lithium-ammonia solutions,  $x_{Li} = 0.1958$  (50 Li and 205 NH<sub>3</sub>). The corresponding experimental densities at 241 K and atmospheric pressure is 0.498 g.cm<sup>-3</sup> leading to side-length of the basic periodic cube of 23.39 Å. Due to the strong screening of the Coulombic interactions by the indirect contributions, cut-off of the total site-site potentials at 12 Å was justified, which saved a significant amount of computer time compared with the Ewald method [Ewald, 1921]. The starting configuration was randomly generated.

## CHAPTER 5

### RESULTS AND DISCUSSION

#### 5.1 Pair Potentials and Pseudopotential Effects

To take into account effect of free electrons in the concentrated lithium-ammonia solution, two models of pseudopotential have been applied. The results obtained from these models representing the site-site interactions are illustrated in Figures 5.1. Total potential,  $V_{tot}^{ij}(R)$ , with  $i, j = \text{H, N, and Li}$  have been calculated according to equation 4.1. Direct potentials,  $V_{dir}^{ij}(R)$ , yielded from the pair potential functions (Table 4.1 and 4.2) and used in previous work [Hannongbua, et al., 1988] have been again employed while indirect potentials,  $V_{ind}^{ij}(R)$ , are calculated from equations 4.5 - 4.14. The total lithium-ammonia and ammonia-ammonia interactions are depicted in Figure 5.2.

It can be seen from Figures 5.1 that, when free electrons are taken into consideration, total site-site potentials are much weaker, less positive and less negative, than the  $V_{dir}^{ij}(R)$ . In Figure 5.2, changes of the lithium-ammonia and ammonia-ammonia potentials which are about 25% and 35%, respectively, are relatively small in comparison with those taken place on the site-site interactions. This fact can be understood as mutual cancellation of the Coulombic interaction [Gurskii et al., 1990]. As can be seen from Figure 5.2, the interaction approaches zero very quickly after the minimum. Therefore, Ewald procedure [Ewald, 1921] which is known to be used to correct an error due to long-range Coulombic effect in computer simulations, was not applied. This leads to the reduction of considerable amount of computer time.

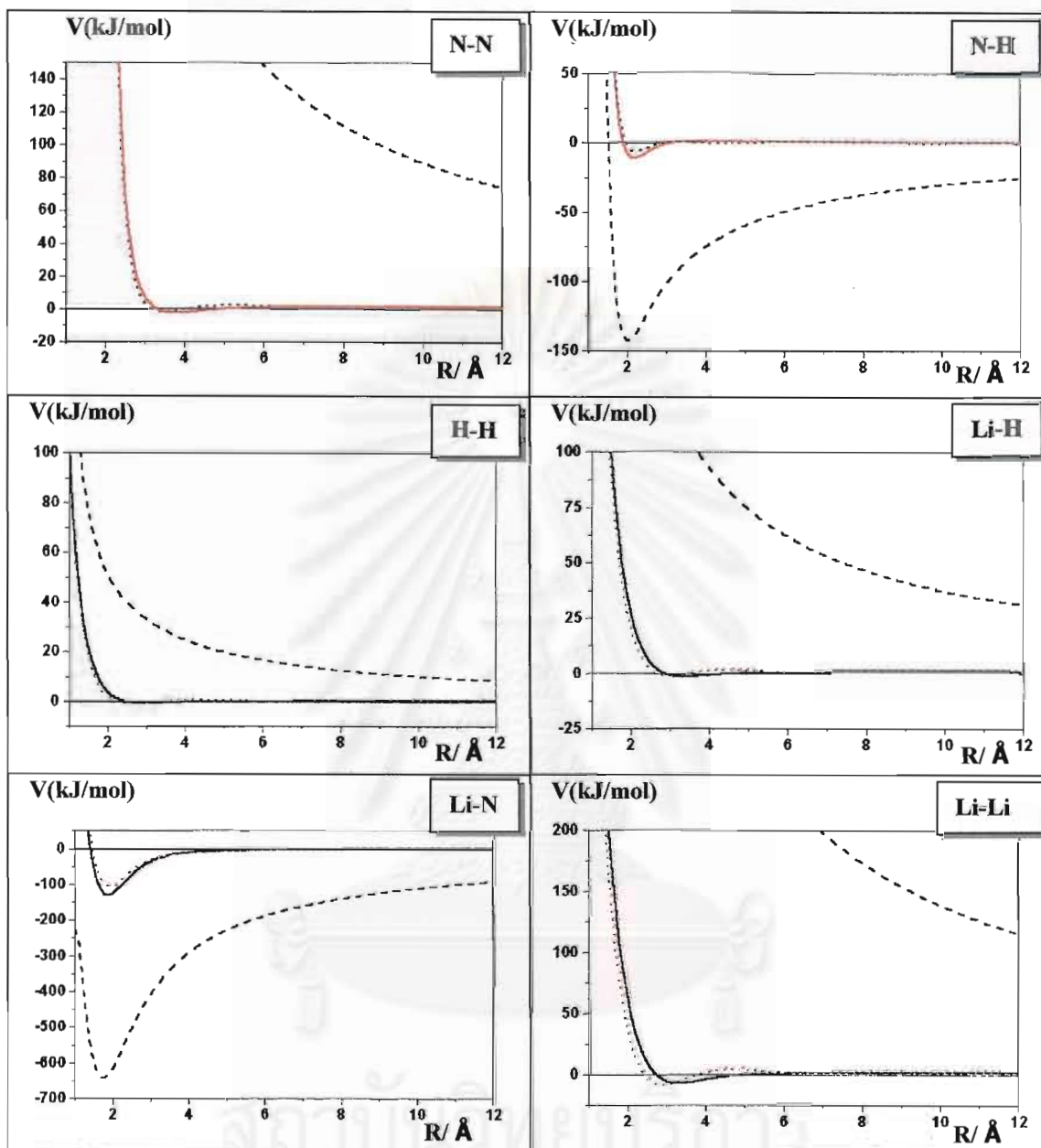


**Figure 5.1** Total site-site potentials as a function of the distances for the six different interactions, calculated from models I (solid line) and model II (dotted line). The dashed line denotes direct interactions.

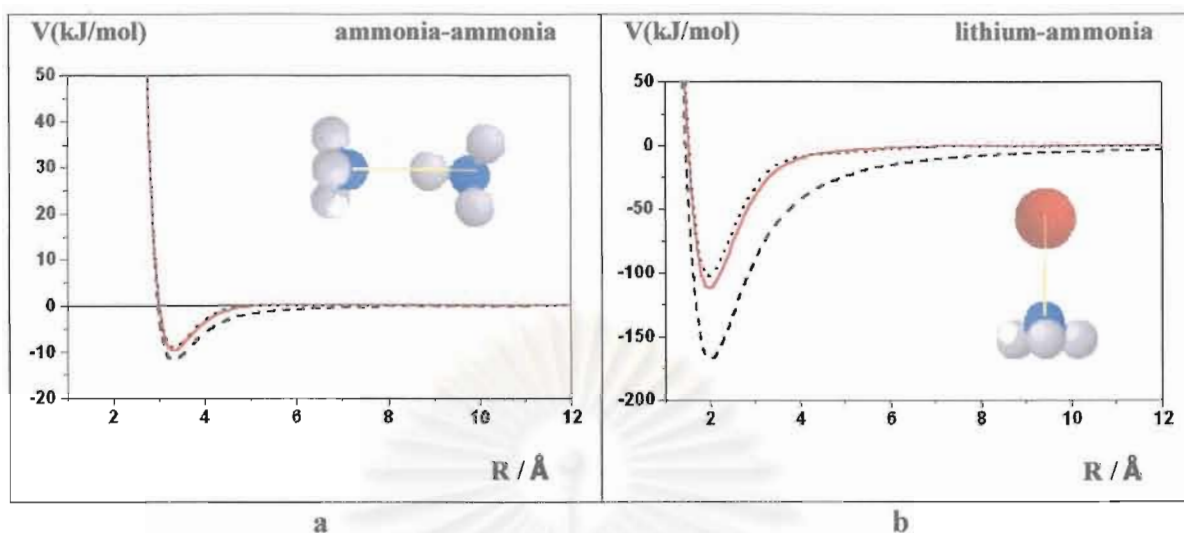


**Figure 5.2** Ammonia-ammonia (a) and lithium-ammonia (b) pair potentials as a function of nitrogen-nitrogen and lithium-nitrogen distances, for the orientations shown in the inserts. The dashed line gives the potential of direct interaction. Solid and dotted lines are the total potentials obtained from model I and II, respectively.

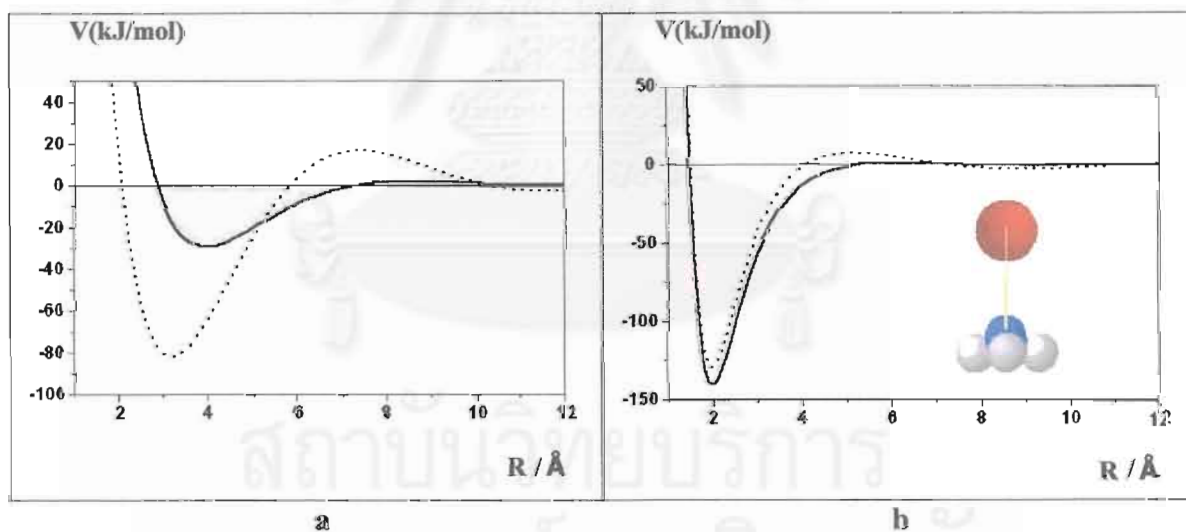


**Figure 5.3** Lithium-lithium (a) and lithium-ammonia (b) pair potentials taken from literatures. Solid lines are from [Hannongbua, et al., 1992] and dotted lines from [Hannongbua, et al., 1997].

Some comments should be made concerning the pseudopotential models used in this work and in the previous works by [Hannongbua, et al., 1992,1997]. Modification is focused on volume of the simulation cube ( $\Omega$ ). An idea is to identify an effective volume where free electrons are able to be occupied in the solution. In the previous works [Hannongbua, et al., 1992, 1997], total volume of the simulation cube has been used without modification. In reality free electrons can not move into certain area which occupied by molecules and ions. Therefore, what is examined in this study is to subtract total volume of the simulation cube by those occupied by ammonia molecules and lithium ions. With this approach, significant changes of the site-site and ion-ammonia interactions have been yielded (Figure 5.2 and 5.3). Comparison with the results obtained from the two models, in terms of the depth and position of the potential minima, both site-site and total (lithium-ammonia and ammonia-ammonia) potentials are not sensitive to the choice of the pseudopotential models used (Figure 5.2). The total lithium-lithium and lithium-ammonia solution applied in this study are much weaker than the previous work while the ammonia-ammonia interaction is not significant different. Note that flexible molecular dynamics simulation is not able to performed in the previous works (molecules are collapsed after certain time steps). The authors conclude that an intramolecular potential for ammonia molecules which derives from experimental data for pure liquid ammonia may not suitable for this solution which contains high concentration of metal ions and free electrons. With the new approach using the effective volume of the simulation cube, flexible molecular dynamics simulation can be smoothly carried out.

## 5.2. Structural Properties

With the time step of  $1.25 \times 10^{-16}$  s, equilibrium was reached after 60,000 and 40,000 time-steps at the average temperature of 241 K and 242 K for the pseudopotential model I and II, respectively. Snapshot of all particles distributed in the simulation cube, one out of 20,000 configurations after equilibrium, is displayed in Figure 5.4.

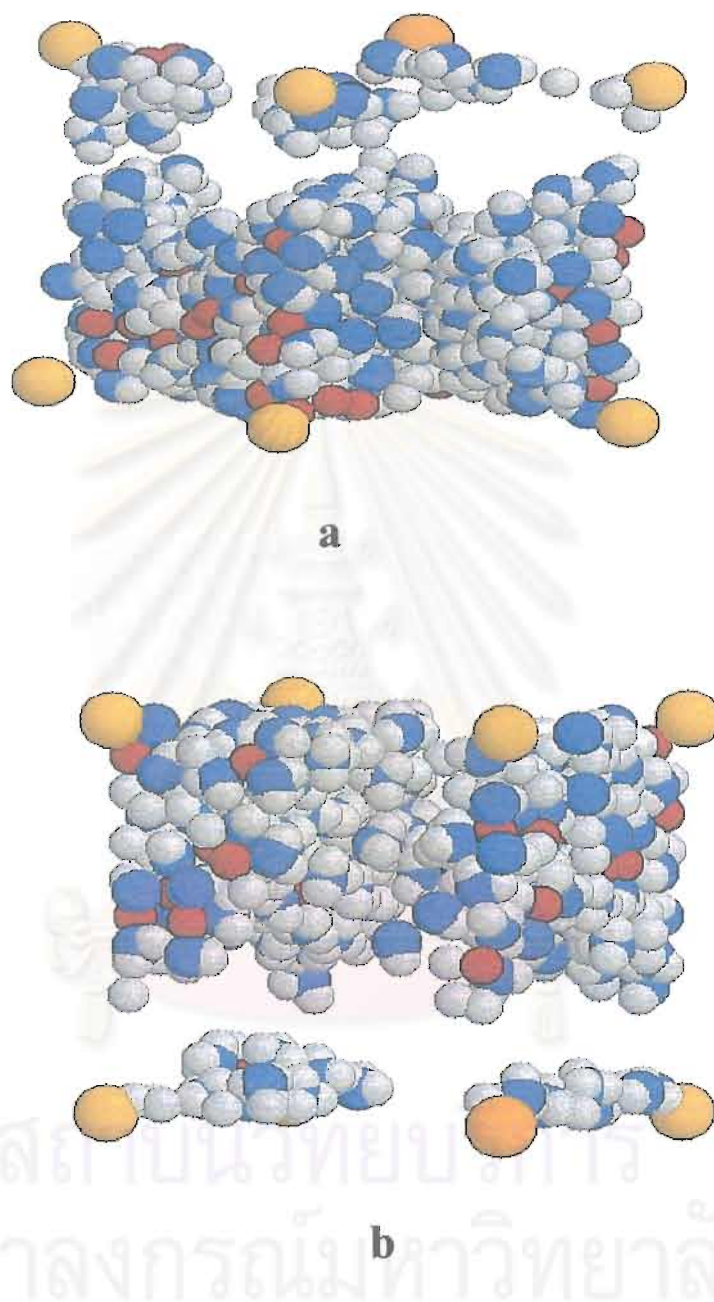


**Figure 5.4** Snapshot of the 19.58 mole percent of lithium ions in liquid ammonia using the pseudopotential (a) model I and (b) model II. The single red balls represent lithium ions. The white together with blue balls denote ammonia molecules (white for hydrogen and blue for nitrogen). The largest orange balls are insert in order to mark the corners of the simulation box.



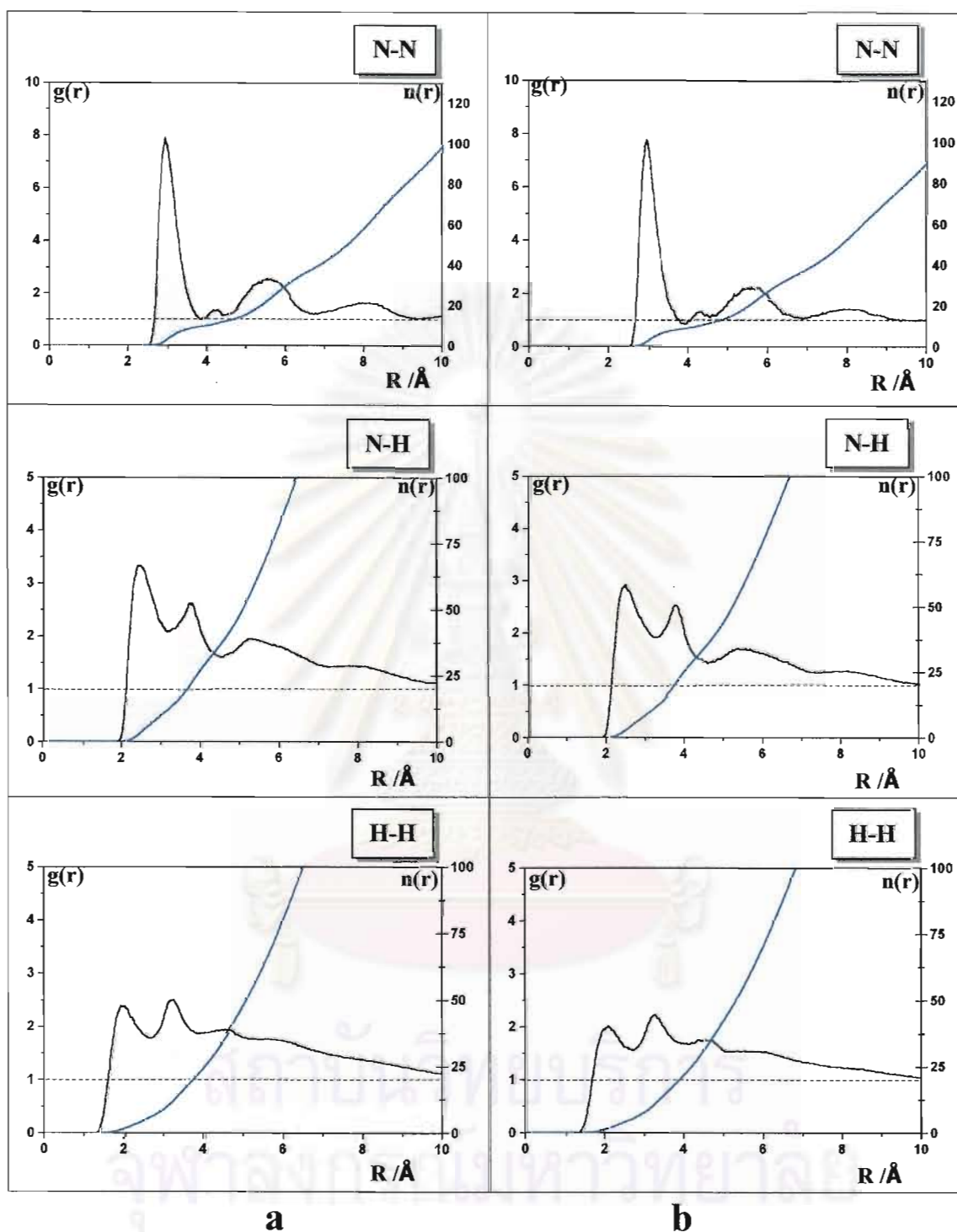


**Figure 5.5** Ammonia-ammonia radial distribution functions and their integration numbers obtained from the simulations using pseudopotential (a) model I and (b) model II.

It can be seen easily from Figure 5.4 that, lithium-ammonia clusters and big cavities are formed in the solution. However more detailed understanding of the solution properties have been investigate in term of radial distribution functions (RDF).

### 5.2.1 Radial Distribution Functions

The ammonia-ammonia RDFs and the corresponding running integration numbers are presented in Figure 5.5. The lithium-ammonia and lithium-lithium RDFs are given in Figure 5.6. No dramatic difference has been significantly found for all RDFs obtained from the two pseudopotential models. Characteristic values as well as those obtained for a single lithium ion in 215 ammonia molecules which is named for convenience as dilute solution [Hannongbua et al., 1988] are summarized in Table 5.1. The coordination number is defined as multiplication between an area under the RDFs (integrated up to the distances beyond their maxima) and number density (number per total volume) of such species. Compare that of dilute solution, shape, distances to all peaks and coordination numbers are completely changed, except those of the Li-N RDF.

Screening effect in the concentrated lithium-ammonia solution reduces strongly the repulsion of the site of the same changes, leading to a much less repulsion of the N-N and H-H interactions (Figure 5.1). These causes, therefore, to more pronounced first peaks of the N-N RDF at about 2.9 Å in comparison to dilute solution. Distance to this maximum is 0.43 Å shorter than that of dilute solution (Figure 5.5 and Table 5.1). This leads consequently the integration number of 8.5 in comparison to that of 12.8 of dilute solution.

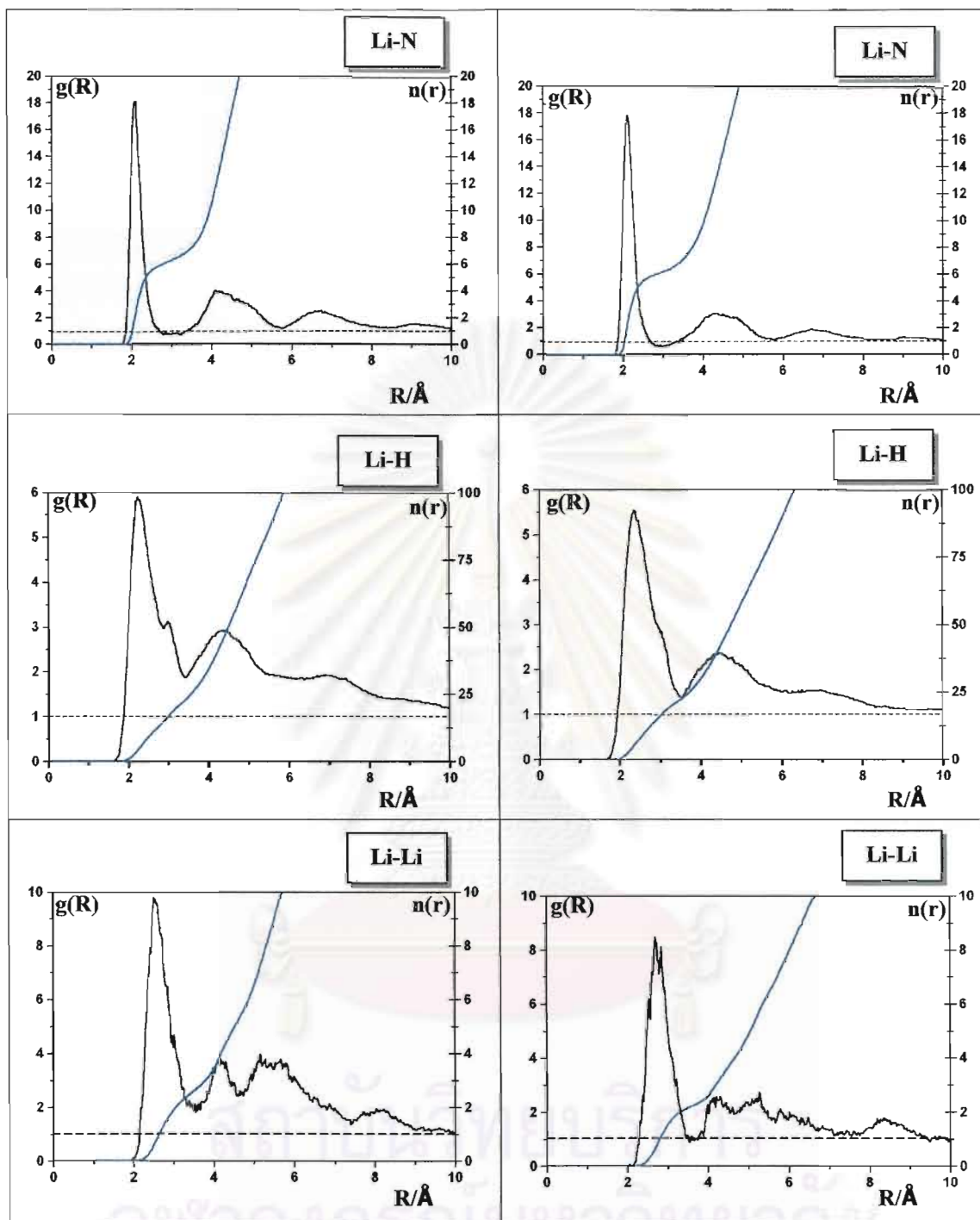
In 19.58 mole percent of lithium ions in liquid ammonia, about four ammonia molecules are available for each lithium ion. While running integration number of the ion obtained from the Li-N RDF are six ammonia molecules in the radius of 2.1 Å. Both coordination number and size of the solvation shell are identical to these obtained from

the simulation of dilute solution (Table 5.1). This result indicates obviously that reduction of the lithium ammonia interaction of about 35% caused by the indirect potential (Figure 5.2) does not effect the lithium solution shell. However, running integration number of six is average from these of 5, 6 and 7 with percentage of 8%, 85% and 7%, respectively.

First peak of the Li-Li RDF is quite pronounced (Figure 5.6) centered at about 2.6 Å. The running integration number is 2.2 integrated up to the first minimum of 3.5 Å. Distribution of Li-Li coordination numbers are given in Table 5.2. This shows that Li cluster of the average size of about 2-3 ions have been formed. Second and third peaks appear at 4.3 Å and 5.5 Å, respectively.

As the two previous works [Hannongbua, et al., 1992] and [Hannongbua, et al., 1997] have to be often mentioned, they will be named work I and II, respectively. In work I, the Geldart-Vosko local field function was used and the 19.58 mole percent lithium ions in liquid ammonia was studied by molecular dynamics simulations. The second one, work II, was studied using Ishimaru local field function for the system consisting of 11.80 mole percent of lithium ions in liquid ammonia by Monte Carlo simulations.

Compare the results obtained from model I of this study (with a smaller effective volume) and previous work I which the same local field function was used for both cases. Distance to the first maximum,  $R_{MI}$ , of N-N RDF of model I is about 0.13 Å longer than that of work I while the Li-Li RDF is about 0.56 Å shorter. The running integration numbers integrated up to the first minimum of the N-N RDF increase from 5.8 to 8.5 in this study while that of Li-Li RDF decrease from 3.0 to 2.2. Consequently, dramatic changes on the N-H and H-H RDFs have been also found. Moreover, the second and third peaks of the Li-Li RDF are clearly appeared for this work but not for the previous work I.



a

b

Figure 5.6 Lithium-ammonia radial distribution functions and their integration number obtained from the simulation using pseudopotential (a) model I and (b) model II.

**Table 5.1** Characteristic values of the radial distribution functions,  $g_{\alpha\beta}(r)$  for the lithium – ammonia solution.  $r_{M1}$ ,  $r_{M2}$  and  $r_{m1}$  are distances in Å where,  $g_{\alpha\beta}(r)$  has first and second maximum and first minimum, respectively,  $n_{\alpha\beta}(r_{m1})$  is running integration numbers, integrated up to  $r_{m1}$ . Those values for the dilute solution, 0.46 mole percent, are also given, in parenthesis, for comparison.

Model I						
$\alpha\beta$	$R_{M1}$	$g_{\alpha\beta}(R_{M1})$	$R_{m1}$	$G_{\alpha\beta}(R_{m1})$	$N_{\alpha\beta}(R_{m1})$	$R_{M2}$
N-N	2.95(3.38)	7.91	3.85(4.29)	0.99	8.5(12.8)	4.27
N-H	2.46(3.62)	3.43	3.49(4.47)	5.2	32.4(34.2)	-
H-H	2.01(3.82)	2.42	2.70(4.56)	4.2	28.3(36.5)	-
Li-N	2.09(2.29)	18.96	2.80(2.88)	0.71	6.0(6.0)	4.01
Li-H	2.22(2.87)	5.89	3.48(3.40)	1.92	18.9(18.0)	4.20
Li-Li	2.64	9.80	3.5	1.89	2.2	4.29
Model II						
N-N	2.89	7.86	3.80	1.03	8.5	4.28
N-H	2.50	2.98	3.51	5.0	30.4	-
H-H	2.09	2.01	3.20	4.4	28.8	-
Li-N	2.15	18.05	2.80	0.97	6.2	4.13
Li-H	2.18	5.72	3.58	1.90	18.9	4.22
Li-Li	2.57	8.30	3.52	0.89	2.1	4.31

**Table 5.2** Percentage of nearest neighbor lithium ions,  $n_{LiLi}(R_{m1})$ , around a central one.

$n_{LiLi}(R_{m1})$	0	1	2	3	4
%	4	16	52	24	5

Although the same local field functions were applied for model II of this study and previous work II, unfortunately they were not possible to be directly compared, because they were performed at different concentrations. However, the results shows, in changing from work II to model II,  $R_{MI}$  of N-N RDF increases from 2.80 Å to 2.89 Å and corresponding integration number decrease from 8.1 to 8.5. First peak of the Li-Li RDF of 2.74 Å of work II reduces to 2.57 Å in this study while their corresponding integration number increase from 0.8 to 2.1.

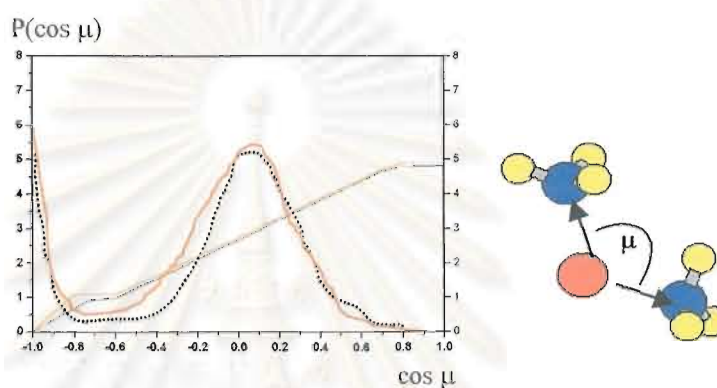


Figure 5.7 Distribution of  $\cos \mu$  ( $\mu$  is defined as the nitrogen-lithium-nitrogen angle calculated) for the ammonia molecules in the solvation shell of the lithium ions. Solid and dotted lines were obtained from model I and II, respectively.

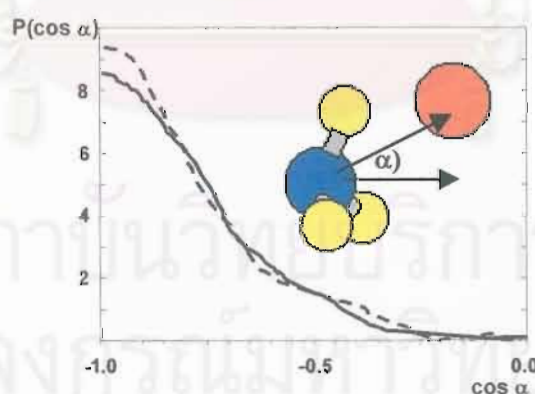
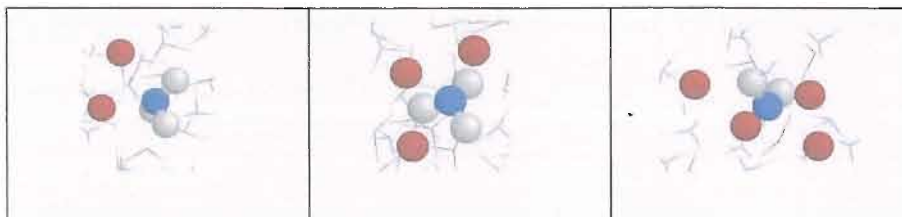


Figure 5.8 Distribution of  $\cos \alpha$  ( $\alpha$  is defined as the angle between the vector parallel to dipole moment of ammonia molecule and the vector pointing from the nitrogen atom toward the lithium ion) for ammonia molecules in the solvation shell of lithium ions. The solid and dashed lines were obtained from the simulations using pseudopotential models I and II, respectively.



**Figure 5.9** Snapshot which show that one ammonia molecule was shared by 2, 3 or 4 lithium ions (nitrogen-lithium distances  $\leq 2.5$  Å). The single red balls represent lithium ions. The white together with blue balls denote ammonia molecules (white for hydrogen and blue for nitrogen).

### 5.2.2 Solvation shell Structure

The geometrical arrangement of the ammonia molecules in the solvation shells of lithium ions can be deduced from the simulation in terms of distribution of  $\cos \mu$  where  $\mu$  is defined as the N-Li-N angle. The result is depicted in Figure 5.7, where only the ammonia molecules in the solvation shells are taken into consideration. Both plot shows two peaks centered at  $88^\circ$  and  $180^\circ$  and the corresponding integration numbers up to the minima beyond the two peak are 1 and 4 ammonia molecule, respectively. This indicates octahedral arrangement of the ammonia molecule around the lithium ions. It is interesting to note that the maximum shifted slightly from an ideal octahedral angle of  $\mu = 90^\circ$  to  $88^\circ$ . This deviation is related to the cluster formation which will be clarified in the next section.

### 5.2.3 Orientation of the Ammonia Molecule

Orientation of ammonia molecule in the solvation shell of the lithium ions is described by the distribution of  $\cos \alpha$ , where  $\alpha$  is defined as the angle between the vector parallel to dipole moment of ammonia molecule and the vector pointing from the nitrogen atom toward the lithium ion. The normalized distributions are presented in Figure 5.8 for both models. The plots show strong preference by pointing the dipole moment of the ammonia molecule pointing away from the ion. Both distributions are

quite broad. This means that in concentrated lithium-ammonia solutions, ammonia molecules in the solvation shell of Li are very flexible.

#### 5.2.4 Cluster Formation

We aim for more understanding in detail of the distribution of ammonia molecules between the solvation shells of lithium ions and the bulk. The different feature of the various RDFs depicted in Figure 5.5 and 5.6 was employed and considered only in solvation shell (Li-N distance is smaller than the position of the first minimum in the Li-N RDFs, 2.80 Å for both models). The coordination number of lithium ion, is found to be six. It has been calculated from the simulation that 20% of all NH<sub>3</sub> belongs to the bulk. From the remaining 80% of molecules, 50% coordinates to one lithium ion and 30% bind simultaneously to more than one lithium ions. In the following discussion we shall denote these three kinds of NH<sub>3</sub> molecules, bind 0, 1 and more than 1 times to the same time, by N0, N1, and N2, respectively. Average size of the clusters consists of 3.2 ions ( $n_{LiLi}$  ( $R_{m1}$ )=2.2).

Next point of interest is the distribution of the ammonia molecules N1 and N2 in the solvation shells of the 50 lithium ions in the solution. With the notation Li(N1)<sub>m</sub>(N2)<sub>6-m</sub>, the calculated results are given in Table 5.3 This data visualize size of the cluster and their distribution in the solution. For instance, only separated octahedrally clusters, Li(N1)<sub>6</sub>, is available. Majority is the cluster of Li(N1)<sub>3</sub>(N2)<sub>3</sub> in which three NH<sub>3</sub> (N2)<sub>n</sub> are shared by the other clusters

**Table 5.3** The fraction in % of the cluster of kind m.

M	6	5	4	3	2
%	4	6	28	40	22



Snapshot plotted in Figure 5.9 demonstrates ammonia sharing. Two, three or four lithium ions were found to coordinate simultaneously to one ammonia molecule. Consequently, big cavities are formed in the solution (Figure 5.4). One believes that this space is where free electron density is concentrated. Also, simulations by Deng, Martyna, and Klein [1992, 1994] demonstrated this behavior, with free electrons move throughout the cavities (Figure 5.10).

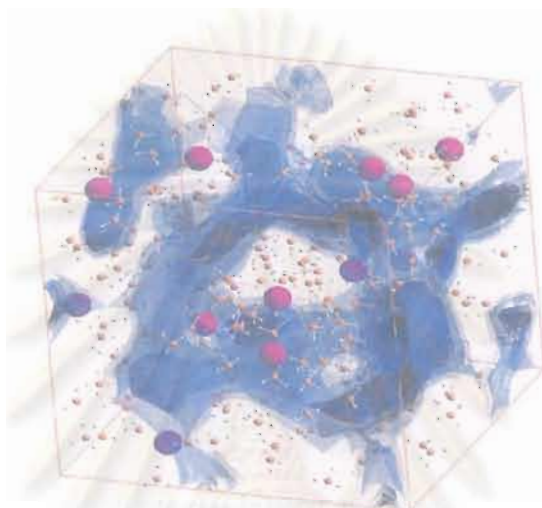


**Figure 5.10** The electron density of a representative configuration of a cesium-ammonia solution at high electron concentration. The system consists of 24 cesium ions in 256 ammonia molecules [Klein 1994].

### 5.3 Dynamical Properties

The dynamical properties of the solution are conveniently calculated from the simulation through time correlation functions. For a system of  $N$  particles, the time dependent autocorrelation function (ACF) of a property  $A$  can be calculated from equation 3.16 – 3.18.

#### 5.3.1 Translational Motions

Translational motions of the molecules can be represented by the velocity autocorrelation function (VACF). The center-of-mass VACFs of the two simulations, model I and model II, both for molecules in the bulk and the first solvation shell have been calculated separately and plotted in Figure 5.11 and 5.12 for model I and II, respectively. The spectral density is defined as

$$\mathfrak{I}(\omega) = \int_0^{\infty} C_v(t) \cos(\omega t) dt ,$$

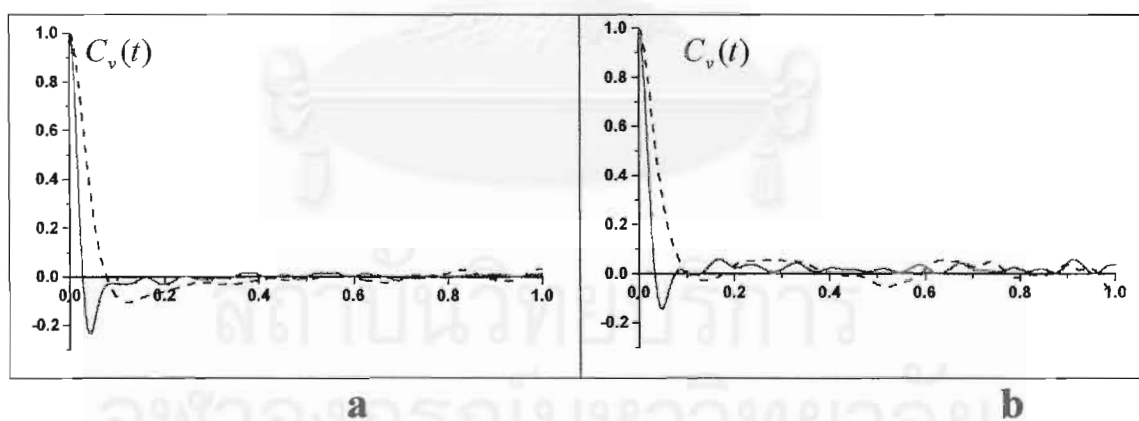


**Figure 5.11** Normalized center-of-mass velocity autocorrelation functions for ammonia molecules in the bulk (dashed line) and in the solvation shell (full line) of lithium for (a) model I and (b) model II.

In Figure 5.11, the normalized center-of-mass velocity ACFs of the ammonia molecules are presented separately for the bulk phase and for solvation shell of the  $\text{Li}^+$ . For bulk ammonia,  $c_v(t)$  decay to zero slower than solvated ammonia for both models. This behavior indicates a relatively free translational motion of bulk molecules that hydrogen bonding plays small role on the structure of the solution. Strong interactions of the ammonia molecules with the lithium ion in its solvation shell lead to pronounced oscillation in the ACFs.

Fourier transform of ACFs shown in Figure 5.11, yields spectral density of the translational motions plotted in Figure 5.12. The plot for bulk ammonia obtained from both models show maximum of about  $100 \text{ cm}^{-1}$ . In the solvation shell, maximum of the spectral density appear at about  $300 \text{ cm}^{-1}$ . The self diffusion coefficient,  $D$ , can be calculated from equation (3.14) for the present simulation at about 241 K. The results are  $2.73263 \times 10^{-5} \text{ cm}^2 \text{ s}^{-1}$ ,  $1.05172 \times 10^{-5} \text{ cm}^2 \text{ s}^{-1}$ , and  $4.25944 \times 10^{-5} \text{ cm}^2 \text{ s}^{-1}$ ,  $1.24148 \times 10^{-5} \text{ cm}^2 \text{ s}^{-1}$  for bulk and solvated molecule yielded from model I and model II, respectively. While  $D$  in the dilute solution are  $9.0 \times 10^{-5} \text{ cm}^2 \text{ s}^{-1}$  and  $1.9 \times 10^{-5} \text{ cm}^2 \text{ s}^{-1}$  for bulk and solvation shell and the experimental one for pure liquid ammonia of  $D = 5.3 \times 10^{-5} \text{ cm}^2 \text{ s}^{-1}$  [Garroway and Cotts, 1997]

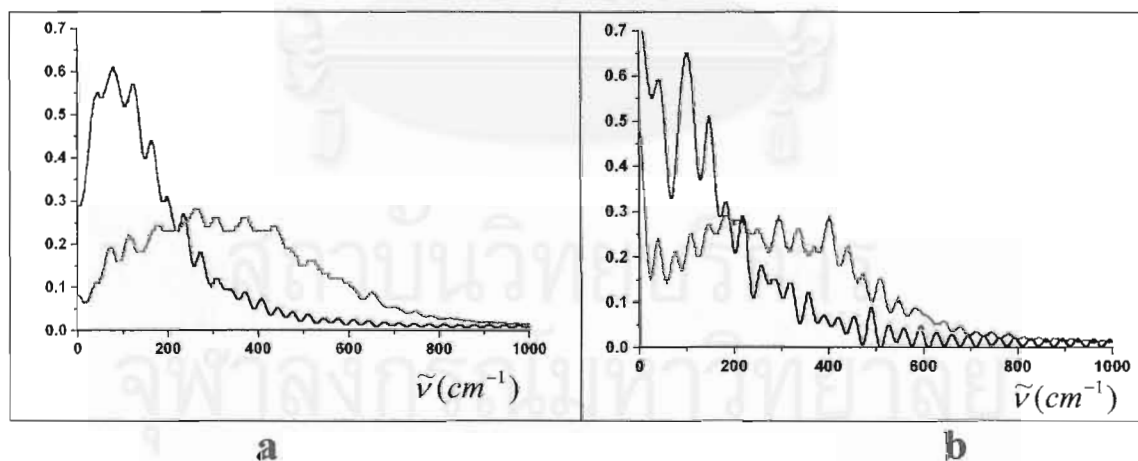


**Figure 5.12** Spectral density of the translational motions of the normalized center of mass velocity autocorrelation functions shown in Figure 5.11 Normalized center of mass velocity autocorrelation functions for ammonia molecules in the bulk (black line) and in the first solvation shell (red line) of lithium obtained from the simulations for (a) model I and (b) model II.

### 5.3.2 Librational motions

Librational dynamics of the ammonia molecules in the simulated system can be studied through the Fourier transform of the ACFs of velocity components of hydrogen atoms. Details of the projections of the velocities onto degenerate axes are explained by Bopp [1986].

The spectral densities of the librational motions of ammonia in the bulk and in the solvation shell of concentrated solutions are presented in Figure 5.13 - 5.14. Frequency of rotation about x-, and y-axes increases from about  $200\text{ cm}^{-1}$  in the bulk to about  $400 - 1000\text{ cm}^{-1}$  in the solvation shell of the lithium ions for both models.

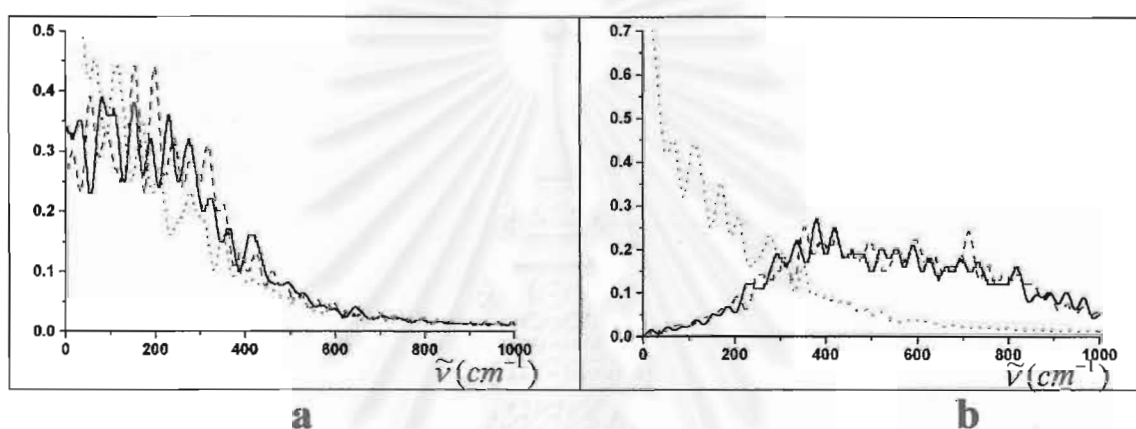


**Figure 5.13** Spectral density of the rotation about x- (full line), y- (dashed line) and z-axes (dotted line) for ammonia molecules in the bulk (a) and in the solvation shell of lithium obtained from model I.

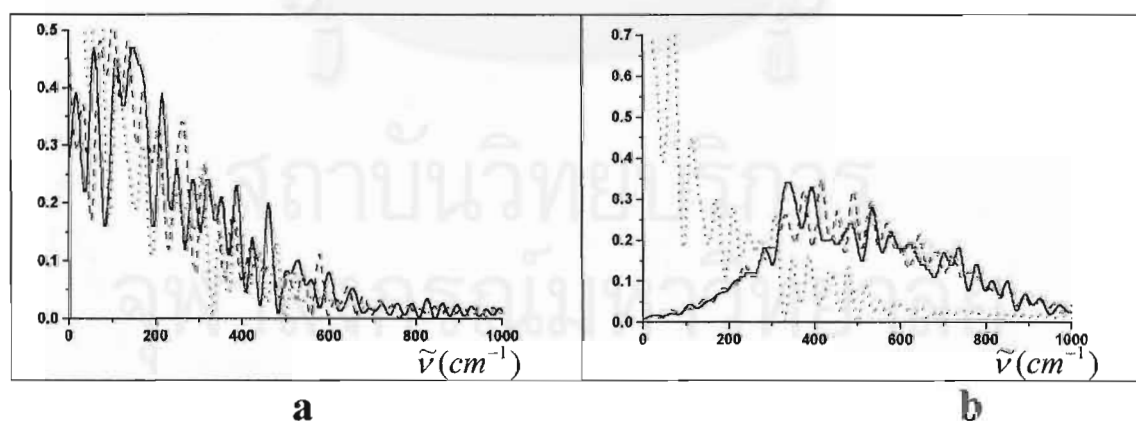


**Figure 5.14** Spectral density of the rotation about x- (full line), y- (dashed line) and z-axes (dotted line) for ammonia molecules in the bulk (a) and in the solvation shell of lithium obtained from model II.

### 5.3.3 Vibrational Motions

Various modes of vibrational frequencies calculated from the simulations of concentrated solutions are shown in Table 5.4, as well as those obtained experimentally. Note that statistical uncertainties in the calculation frequencies are approximately  $\pm 20 \text{ cm}^{-1}$ . The vibrational frequencies from experiments and from simulations are consistent. Qualitative agreement of the vibrational frequency of the bulk molecules indicates the quality of the potential used. The spectral calculated for asymmetric stretching and bending shown in Figure 5.15.

**Table 5.4** Comparison of various vibrational frequencies calculated from the simulation separately for ammonia molecules in the first solvation shell of lithium ions, the bulk liquid, and in the gas phase with experimental results.

	MD(Li <sup>+</sup> - NH <sub>3</sub> )		Pure ammonia (experiment data)	
	Solvation shell model I/II	Bulk liquid model I/II	Liquid <sup>†</sup>	Gas <sup>*</sup>
Sym. Bend.	1160/1150	1125/1130	1066	932, 968
Asym. Bend.	1620/1640	1630/1650	1638	1627
Sym. Stretch.	3200/3250	3250/3300	3240	3336
Asym. Stretch.	3330/3350	3320/3340	3379	3444

[Birchall 1970] <sup>\*</sup>[Spirko 1983].

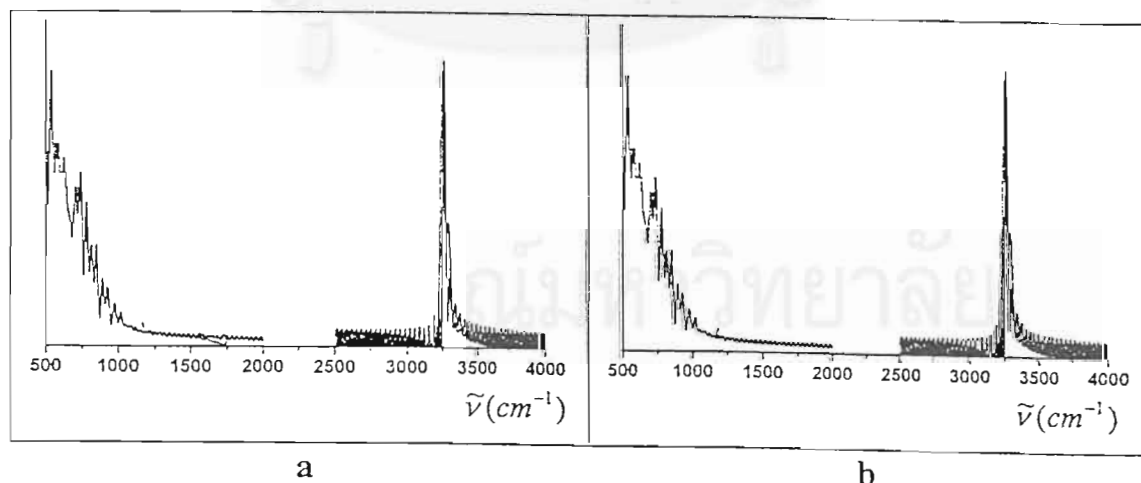


**Figure 5.15** Asymmetric stretching and bending spectral densities obtained from the simulation using pseudopotential (a) model I and (b) model II.

## CHAPTER 6

### CONCLUSION

With the approach suggested here, computer simulation techniques developed for classical systems have been used to investigate the system consisting of free electrons.

#### 6.1 Potential Functions

The total potential which describes the effective interaction for all particles in the flexible MD simulations consists of 2 parts namely inter- and intramolecular potential functions, Interaction between sites of kind  $i$  and  $j$  in metal ammonia system containing free electrons is given by summation between  $V_{dir}^{ij}(R)$  and  $V_{ind}^{ij}(R)$ . Where  $V_{dir}^{ij}(R)$  is the direct interaction and  $V_{ind}^{ij}(R)$  is the change of the direct interaction due to the presence of free electrons. The  $V_{dir}^{ij}(R)$  is usually developed using quantum chemical calculations while the  $V_{ind}^{ij}(R)$  was calculated using pseudopotential method. The total potential becomes generally much weaker than  $V_{dir}^{ij}(R)$ .

#### 6.2 Structural and Dynamical Properties

The results from the simulations using two models of pseudopotential show that lithium ion was solvated by six ammonia molecules. Solvent structure was completely changed in comparison with those observed for pure liquid ammonia. Big clusters of  $Li_m(NH_3)_n^+$  and share of one ammonia molecule by 2 and 3 lithium ions has been detected. As a consequence of the cluster formation, big cavities are formed

in the solution. Once believes that this space is where the electron density is concentrated.

### 6.3 Suggestions for Further Study

Some comments and suggestions for further study are the following.

- As it was found somehow that structural and dynamical properties obtained from the two models in this study and from the previous works [Hannongbua et al., 1992, 1997] are not sensitive to the pseudopotential used. It is possible that structure of the solution is too tight, especially the lithium-ammonia clusters. However, it is suggested to modify the available models or to find the other models of pseudopotential which yield weaker binding.
- It would be very interesting to perform simulation using temperature dependent pseudopotential. The results, especially diffusion coefficient and vibrational spectra can be directly compared to series of experimental data which are available in the literature [Garroway and Cotts, 1973]. In this case, an intramolecular potential for ammonia molecules would be newly developed, using experimental data at high concentrated solution, not from pure liquid ammonia as it is used before.

## References

- Alder, B. J. and Wainwright, T. E. 1957. **J. Chem. Phys.** 27: 1208.
- Alder, B. J. and Wainwright, T. E. 1959. **J. Chem. Phys.** 31: 459.
- Bopp, P. 1986. **Chem. Phys.** 196: 205.
- Born, M. and Karman, V. 1912. **Physik. Z.** 13: 297.
- Born, M. and Oppenheimer 1927. **Ann. Physik.** 84: 457.
- Boys, S. F. 1950. **Proc. Roy. Soc. A** 200: 542.
- Boys, S. F. and Bernardi, F. 1970. **Mol. Phys.** 19: 553.
- Dang, L. X. 1992. **J. Chem. Phys.** 96: 6970.
- Deng, Z., Martyna, G. J., and Klein M. L. 1992 **Phys. Rev. Lett.** 68: 2496.
- Deng, Z., Martyna, G. J., and Klein M. L. 1994 **J. Chem. Phys.** 100: 7590.
- Ewald, P. P., 1921. **Ann, Phys.** 64: 253.
- Frenke, D. and Smit, B. 1996. **Understanding Molecular Simulation.** CA: Academic Press.
- Frenkel, J. 1946. **Kinetic theory of liquids.** Oxford: Clarendon Press.
- Garroway, A. N. and Cotts, R. M. 1973. **Phys. Rev. A** 7: 635.
- Gurskii, Z., Hannongbua, H., Heinzinger, K. 1993. **Mol. Phys.** 78: 461.
- Hannongbua, S. 1991. **Aust. J. Chem.** 44: 447.
- Hannongbua, S. 1997. **J. Chem. Phys.** 106: 6076.
- Hannongbua, S. 1998. **Chem. Phys. Lett.** in press.
- Hannongbua, S. V., Ishida T., Spohr, E., and Heinzinger, K. 1988. **Z. Naturforsch.** 43a: 572.
- Hannongbua, S., Kerdcharoen, T., and Rode, B. M. 1992. **J. Chem. Phys.** 96: 6945
- Harrison, W. 1963. **Phys. Rev.** 131: 2433.
- Ichimaru, S. and Utsumi, K. 1981. **Phys. Rev. B** 24: 7385.



- Impey, R. W. and Klein, M. L. 1984. **Chem. Phys. Lett.** 104: 579.
- Jansen, L. 1962. **Phys. Rev.** 125: 1798.
- Kelterbaum, R., Turki, N., Rahmouni, A., and Kochanski E. 1994 **J. Chem. Phys.** 100: 1589.
- Klein, M. L. 1994. <http://www.psc.edu/MetaCenter/MetaScience/Articles/Klein/Klein.html>  
University of Pennsylvania, Michael L. Klein.
- Metropolis, N., Rosenbluth, A. W., Rosenbluth, M. N. Teller, A. H. and Teller, E. 1953. **J. Chem. Phys.** 21: 1087.
- Narten, A. H. 1977. **J. Chem. Phys.** 66: 3117.
- Nasby, R. D. and Thomson, J. C. 1970. **J. Chem. Phys.** 53, 109.
- Onsager, L. 1936. **J. Am. Chem. Soc.** 58: 1486.
- Roothaan, C. C. J. 1951. **Rev. Mod. Phys.** 23: 69.
- Sagarik, K., Ahlrichs, R., and Brode, S. 1986. **Mol. Phys.** 6: 1247.
- Schroeder, R. L., Thompson, J. C., and Oertel, P. L. 1969. **Phys. Rev.** 178: 298.
- Sidthisoradej, W. 1997. **Ph.D. Dissertation.** Chulalongkorn University.
- Slater, J. C. 1930. **Phys. Rev.** 35: 509.
- Spirko, V. 1983. **J. Mol. Spectrosc.** 101: 30.
- Strett, W. B., Tildesley, D. J., and Saville, G. 1978. **ACS Symp. Ser** 86: 144.
- Thompson, J. C. 1976. **Electron in Liquid Ammonia.** Oxford: Clarendon Press.
- Tongraar, A., Hannongbua, S., and Rode, B. M. 1997. **Chem. Phys.** 219: 279.
- Weast, R. C. 1976. **Handbook of Chemistry and Physics.** 57th ed., Ohio: CRC.
- Weyl, W. 1864. **Poggendorffs Annln.** 121: 601.
- Whitten, J. C. 1963. **J. Chem. Phys.** 44(1): 359.
- Yongyai, Y., Kokpol, S., and Rode, B. M. 1991. **Chem. Phys.** 156: 403.

## Appendix



สถาบันวิทยบริการ  
จุฬาลงกรณ์มหาวิทยาลัย

## Appendix

### Molecular Dynamics Program Structure

#### MAIN

The program structure of MAIN program is shown in Figure A.1. This routine is control other routine and simulation done.

```
PROGRAM MAIN

INCLUDE PARCOM
INCLUDE LVFCOM

CALL INPUT
CALL CONSTANT

CALL PSEU
CALL PSEUWRT
CALL PSEUREAD

CALL POWTPRP
CALL OUTPUT
CALL HISTSTRT

DO 10 LOOP = 1, NTSTEP
  IF (MOD(LOOP,100).EQ.1) CALL NEBR
  CALL POWT
  CALL PRED
  CALL CORR
  CALL RUNTEST
  IF (MOD(LOOP,10).EQ.1) CALL HISTOUT
10 CONTINUE

CALL HISTEND

STOP
END
```

**Figure A.1** Procedural detail of MAIN program.

**PARCOM & LVFCOM**

These parts are stored all sharing variables which used in program's routines.

**CONSTANT**

The physical constants and widely used variables are set in this subroutine.

**INPUT**

This routine read all information necessary to perform the simulation from the input file, and convert them to unit used in the program.

**PSEUDO**

The routine used for calculate the indirect interaction function,

$$V_{ind}(R) = \frac{\Omega_0}{\pi^2} \int_0^\infty F(q) \frac{\sin qR}{R} q dq$$

$$F_{ind}(R) = - \frac{d \left( \frac{\Omega_0}{\pi^2} \int_0^\infty F(q) \frac{\sin qR}{R} q dq \right)}{dR}$$

**PSEUDOWRT**

This routine writes indirect interaction and indirect force into table.

**PSEUREAD**

This routine reads indirect interaction and indirect force from table.

**POWTPRP**

Since the shift-force potential method have been applied to the intermolecular interaction calculations, the necessary value used in the method were prepared in thin subroutine.

## OUTPUT

This subroutine simply writes the data used in program to an appropriate output files.

## HISTSTRT

The actual simulation begin with reading the starting configuration, positions and velocities, from configuration file, performing by this HISTSTRT subroutine.

## NEBR

Since potential and the forces become zero beyond the cutoff distance, due to shift-force potential method. Only the neighbor on the distance not longer than cutoff radius need to account in calculation. This subroutine count for the neighbor list, containing a list of effective particles, and update them at specified intervals.

## POWT

The force and potential on each particles in simulations system are calculated in this subroutine. Each pairs of interaction were calculated by the specific subroutines called by this subroutine.

## PRED

The predicted  $\vec{r}(t)$ ,  $\vec{v}(t)$ ,  $\vec{a}(t)$ , and  $\vec{b}(t)$  for the next timestep of nitrogen atoms, hydrogen atoms and calcium ions were calculated in this subroutine. The periodic boundary conditions were also taken care.

## CORR

after the predicted  $\vec{r}(t)$ ,  $\vec{v}(t)$ ,  $\vec{a}(t)$ , and  $\vec{b}(t)$  have been calculated, they were corrected in this subroutine.

## RUNTEST

This routine is used for observed any properties the simulations system and insert required condition into the system. Any subroutine used for observe and for control system properties were attached with this routine.

**HISTOUT**

At every specified timesteps, this routine write the system configuration, positions and velocities to the history files for later used.

**HISTEND**

Before the program terminated normally, this routine write the system last configuration, positions and velocities to the appropriate files for later used.



จุฬาลงกรณ์มหาวิทยาลัย

## CURRICULUM VITAE

Tawun Remsungnen

- 1974 Born July 6<sup>th</sup> in Nakorn Rachasima, Thailand  
 Father: Mr. Bumroong Remsungnen  
 Mother: Mrs. Chalaem Remsungnen
- 1980-1984 Elementary School (Tesabal Samakee Vitaya, Mahasarakham)  
 1984-1987 Elementary School (Tesabal Burapha Vitayakarn, Mahasarakham)
- 1987-1993 High School (Sarakham Pittayakom, Mahasarakham)
- 1993-1997 Bachelor Of Science (Chemistry),  
 Khon Kaen University, Khon Kaen
- 1997-1999 Master's degree student in Computational Science  
 Faculty of Science, Chulalongkorn University, Bangkok



สถาบันวิทยบริการ  
 จุฬาลงกรณ์มหาวิทยาลัย